Fall 2016

Study and development of robust preformed particle gels for conformance control

Yifu Long

Department:

STUDY AND DEVELOPMENT OF ROBUST PREFORMED PARTICLE GELS FOR CONFORMANCE CONTROL

by

YIFU LONG

A THESIS

Presented to the Faculty of the Graduate School of the

MISSOURI UNIVERSITY OF SCIENCE AND TECHNOLOGY

In Partial Fulfillment of the Requirements for the Degree

MASTER OF SCIENCE

in

PETROLEUM ENGINEERING

2016

Approved
Dr. Baojun Bai, Advisor

Dr. Ralph Flori

Dr. Shari Dunn-Norman

ABSTRACT

To improve the oil recovery of mature reservoirs, technologies referring to conformance control have been widely developed and implemented. Among various technologies, preformed particle gel (PPG) treatment has attracted increasing attentions. PPGs, as a kind of deformable plyometric superabsorbent, could be pumped through injection wells as plugging agents to block the fracture or high-permeability zone in a reservoir.

In decade usage of PPGs, an intensively employed material is poly(acrylamide) (PAM) based hydrogel. However, conventional PAM gel did reveal deficient in formidable conditions, such as formations with high temperature and high salinity. Therefore, a novel PPG based on starch-grafting-poly(acrylamide)/nano-composite (SAC) hydrogel has been designed and successfully synthesized. Starch was utilized to improve viscoelasticity thereby facilitate particles' retention in fractures. Nano-clay was introduced to promote not only gel's strength but also its thermal stability. Optimization of components and analysis of environmental sensitivity were conducted via investigating gel swelling ratio and rheological property in which gel's viscoelasticity was quantified through HAAKE Rhescope1 rheometer. Core-flooding tests were performed using fractured sandstone core as physical simulation models to study the plugging performance of SAC gels in fracture media.

According to experimental results, SAC gel was turned out an overwhelming PPG material compared with conventional PAM gel.

ACKNOWLEDGMENTS

First and foremost, I would like to express my deepest gratitude to my advisor, Dr. Baojun Bai, for his guidance throughout the study of my master degree. His, dedication, erudition and diligence encourages me to become a better learner, and a better researcher.

I would like to appreciate my committee members, Dr. Ralph Flori and Dr. Shari Dunn-Norman for their valuable advice hand comments.

I wish to extend my thanks to United States Department of Energy (DOE), ConocoPhillips Co., Occidental Petroleum Corporation (OXY), and Daqing Wantong Chemical Plant for their funding to this project.

I would like to send my sincere gratitude to Dr. Lizhu Wang and Dr. Thomas Schuman, for their patient guidance. In addition, I want to thank all of my colleagues, Dr. Zun Chen, Ze Wang, Jingyang Pu, Jiaming Geng, Changqian Zhu, Haifeng Ding, Xindi Sun, Sujay Suresh, Yashu Chen, Adriane Melnyczuk for their help.

I would like to show my inmost gratitude to my parents. Thank you for their spiritual and economic support.

TABLE OF CONTENTS

LIST OF ILLUSTRATIONS

Page

LIST OF TABLES

Page

1. INTRODUCTION

Excessive water-production is acknowledged as the most significant problem in the development of mature oilfield. Among various remediation aiming at water-production control, gel treatment has been proven one of the most cost-effective approaches. In term of gel treatment, a well-designed amount of liquid-based or colloid-based polymeric agent will be pumped into the target zone to seal or block the thief-zone which was comprised by fractures or high-permeability channels. Herein, instead of being produced, the injection water will be diverted towards the unswept zone where is rich of remaining oil [45]. Since the first successful operation in 1985[46], technologies regarding gel treatment have boosted, accordingly, they were categorized based on different treating materials, involving in-situ gel, preformed particle gel (PPG), and micorgel treatments [47]. Nevertheless, in-situ gel treatment was widely implemented, this technology possessed its inherent defects. Since the gelant was injected as a form of liquid and the gelation occurred in subterranean, gelation time and gel quality will be strongly interfered by dilution, shear-thinning and chromatography [48]. Meanwhile, the applications of microgel or nanoparticles have been limited by its high cost of manufacture. In contrast, PPG treatment, the technology which overcame those drawbacks, is becoming increasingly attractive for both researchers and industrial engineers.

In decade usage of PPGs, poly(acrylamide) (PAM) or poly(acrylamide-co-acrylate) performed the major component for these particulate hydrogels. In spite of its versatile performance, conventional PAM gels were also found prone to ‘extrusion’ due to its poor mechanical and rheological performance[49][50]. Extrusion was a negative phenomenon implying the plugging agents were too weak to withstand high pressure difference, which always resulted in an ineffective remediation for large fractures or Super-K channels [12].

Accordingly, it would be advantage of introducing starch to improve the viscoelasticity of hydrogel. Starch is an abundant biopolymer which could be found from all complex plants in varying degrees [57]. It is hardy and resistant to most types of chemicals and relatively stable at moderate temperature [14]. Before employed for

enhanced oil recovery (EOR), the applications of starch as the raw material for oilfield polymeric additives began with fluid-loss control and shale stabilization[58][59]. Then, its unique structure and reactivity opened up the possibility for designing plugging agent based on this polysaccharide. In 1998, Maria et al. reported modified starch crosslniked by organic and inorganic crosslinkers which could function as water shutoff agent [61]. Hou and his group members did extensive work with in-situ starch gel in which the gelant was comprised by modified starch, monomer, crosslinker and initiator [51][62]. Ru studied the gelation effect performed by cationic starch and negatively charged, hydrolyzed poly(acrylamide) (HPAM), via electrostatic attraction[63][64]. Although numerous starches and their derivatives have been prepared and studied, as far as we know, this versatile additive has not been introduced to particulate gel.

A successful gel treatment always required hydrogel to be durable and long-termed thermal stabile. In subterranean formation, the acrylamide moiety in conventional PPG underwent substantial hydrolysis when subjected to high temperature. Consequently, the formation of a more hydrophilic pendant, carboxylate group, was accelerated, thus not only rendered PPG an excessive swelling but also resulted in viscoelasticity deteriorated. Given this, it is of critical essentiality to highlight the gel thermal-stability both in gel optimization and evaluation. A viable approach to promote the thermal-stability was surface nonorganic-modification via nano-composite technology [53][54][55]. To execute this nonorganic-modification, a type of nano sized clay, nano Na-MMT, was exploited with the method *in-situ* polymerization. Beyond the enhancement of thermal-stability, another benefit of using nanoclay might be that this nanoscale particle was able to function as '*physical crosslinker',* by which the viscoelasticity of hydrogel would be improved [65][66]. To be noted, in our work *starch grafting* polymerization and *in-situ* polymerization were combined together, targeted in developing a robust hydrogel for PPG treatment in the formidable reservoir conditions.

Beyond nanocomposite technology, another technology, interpenetrating polymer network (IPN), was utilized to increase the mechanical properties of hydrogel. Compared with PAM gels, PVA hydrogel is an inexpensive material which has non-toxicity, bio-compatibility and lower hydrophilicity, most importantly, it has better resistance to pH-changing, salinity, temperature and a high mechanical strength capability, which enable it

be incorporated into other polymer hydrogels to improve their mechanical properties as an environment friendly modifier. PVA has been incorporated into PAM hydrogel to make PAM/PVA composition, and achieve a promotion in acid, salt- resistance as well as mechanical strength, rendering this hydrogel can work under harsh acidic or briny environment.

Two methods have been reported to incorporate PVA into other hydrogels: (1) Polymerizing/ crosslinking water soluble monomers/polymers in PVA solution. In this method, water soluble monomers or polymers and their crosslinker were dissolved in linear PVA solution, and in-situ polymerization/crosslinking reaction happened after adding initiator. This method is a kind of physical mixing first, through polymerizing and crosslinking acrylamide, linear PVA was entangled and embedded in gel matrix without further crosslinking, thus these kind of network structure is called semi-IPN. (2) Polymerizing/crosslinking water soluble monomers/polymers in PVA solution, following by freeze-thaw crosslinking of PVA. Other than the first polymer network, this method prepared the second crosslinking network by creating hydrogen bonding as physical crosslinking points between PVA polymer chains. This kind of IPN only stably existed in moderate environment due to the disrupting of hydrogen bonding under elevated temperature (45~55 ℃). When stimuli applied, such physical crosslinking points may disappear to form semi-IPN. For semi-IPN un-crosslinked PVA could be released in environmental aqueous solution probably.

In this study, a series of PVA/PAM IPN hydrogels containing various amounts of PVA were prepared by in situ free radical solution polymerization of AM and MBA, as well as chemically crosslinking of PVA by glutaraldehyde. Different from physical mixing/entanglement or hydrogen bonding crosslinking point, covalent bonding between PVA polymer chains was more stable under shearing. After permanent incorporation of PVA, the mechanical properties of the swelled three dimension networks have been promoted obviously. Swelling performances of the hydrogels in brine were measured. Rheological and mechanical properties were determined and discussed as well.

2. ROBUST HYDROGELS AND POTENTIAL TECHNOLOGIES FOR CONFORMANCE CONTROL: A LITERATURE REVIEW

2.1. BACKGROUND OF GEL TREATMENT

After the depletion of natural energy for primary recovery, there is an inevitable need of maintaining the reservoir pressure. Water flooding, as the most practical approach of secondary recovery, has been widely implemented to maintain reservoir pressure and displace remaining oil. After 10 percent of reservoir's original oil in place (OOIP) being produced by primary recovery, secondary recovery could extend an increment production of 20 to 40 percent of OOIP [17]. So far, only one-third of the oil (377 billion barrels) have been recovered by conventional primary and secondary methods in the United States. Despite of that most of the easy-to-produce oil have been recovered from U.S. oil fields, enhanced oil recovery (EOR) technologies offer prospects for extracting more oil from these mature oil fields.

EOR technologies are often implemented after secondary recovery to produce more hydrocarbon from the reservoirs. EOR technologies can be classified into four major categories: thermal recovery, chemical flooding, gas injection and microbial method. These processes are intended to improve the sweep efficiency, reduce the residual oil saturation and thus increase the incremental oil production. According to the report from Department of Energy, there is a potential of producing 688 billion barrels by EOR by 2030.

Conformance is the management and alteration of water and gas flows measuring the uniformity of the flood front of the injected drive fluid during an oil recovery flooding operation. Conformance control, as any action to enhance the injection or production profile of a well, includes the procedures that improve both recovery efficiency, wellbore integrity and stratify environmental regulations. Generally, conformance control can be divided into two main categories: mechanical method and chemical method which involved gel treatment, resin treatment, and cement treatment.

Gel treatment has been proven a cost-effective method which can assist in reducing excessive water production and correct reservoir heterogeneity [18]. The objective of the gel treatments in injection wells is to reduce water flow through the *thief zone*, and divert the injected fluids toward the low permeability zone or unswept zone. In

the production wells, gel treatment is adopted to reduce water production without impairing oil production. Known as water shutoff technology, gel treatment applied in production wells highlights *disproportionate permeability reduction* (DPR), which functioned in different manners, compared to the gel treatment in injection wells. This work focused on the content regarding gel treatments in injection wells, namely profile control or profile modification.

Gel treatments could be classified as *in-situ gel treatment* and *preformed particle gel* (PPG) *treatment* according to different conditions where gelations occur, subterranean or superterrene. During in-situ gel treatment, gelant that mixed by polymer solution and crosslinker was injected to target formation, while the gelation occurred under reservoir temperature [24], forming a bulk gel that can fully or partially seal the formation. A newer trend in gel treatment is an application of PPGs in which gels were formed at surface facilities prior to their injection into a reservoir.

PPGs can overcome some inherent drawbacks of in-situ gelation systems, such as the uncertainty of gelation time, unfavorable gelling interfered by shear, change of gelant compositions and dilution by formation water. There are different commercially available PPGs, such as *preformed bulk gels* [25] *partially performed gels* [25], *pH-sensitive cross linked polymer* [26] [27], *microgels* [28] [29] [30], swelling micron-sized polymers such as Bright Water® [31] [32] and micrometer to millimeter sized PPGs [33] [34] [35]. Major differences among these particle gels exist in their particle size, swelling ratio and swelling kinetic.

Published documents showed that microgels and submicron-sized polymers PPGs have been applied economically to reduce water production and improve oil recovery in mature oil fields. Microgels have been applied to approximately 10 gas storage wells to reduce water production [30]. Submicron-sized particles have been applied to more than 60 wells [36] [37]. Additionally, swelling gels were successfully implemented to control CO_2 breakthrough in CO_2 enhanced oil recovery project [38].

Millimeter-Sized PPGs have been applied to over 5000 wells in water floods and polymer floods in China [39]. Millimeter-sized PPGs are used mainly for reservoirs with fractures or fracture-like channels that have a permeability of more than a few Darcies. Therefore, millimeter-sized PPGs cannot penetrate into conventional porous media

without fractures and voids, but they can plug fractures or high-permeability streaks/ channels in mature oilfields which cannot be accomplished by in-situ gels, microgels and sub-micro gels [39].

Table 2.1. Major types of preformed particle gels.

Name		Developer	Particle size	Applications
Preformed Particle Gels (PPG)		Missouri S&T, Halliburton and PetroChina	Millimeter (10 μm to mms)	More than 5,000 injection wellls
Microgel and nanoparticle	Microgel	IFP	Micrometer (1-10 μm)	More than10 production wells
	Brightwater®	Chevron, BP and Nalco	Sub-Micrometer (< 1 μm)	More than 60 injection wells
	pH sensitive microgel	UT Austin	Micrometer (1-10 μm)	N/A

2.2. SYNTHESIS AND FABRICATION OF GELS

Gels are crosslinked three-dimensional (3D) networks, absorb solvents, and swell to a limited degree without dissolution wherein crosslinking is to establish junction between different chains. Thus, the crosslinking methods perform a significant role for gel properties.

In the creation of network structures by chemical bonding, there is a method of: (1) crosslinking at the same time as polymerization; or (2) crosslinking by chemical reaction after the formation of linear polymer chains. Accordingly, a precursor of gels can be a monomer (water-soluble or oil-soluble monomer), a polymer (natural or synthetic polymers), or a monomer and polymer mixture. Using monomer as raw material, there are several polymerization methods, nevertheless, only two routes are commonly employed for gel preparation regarding gel treatment. They are solution

polymerization and emulsion polymerization. Based on the purpose of this work, we will emphasize solution polymerization rather than emulsion polymerization.

2.2.1. Crosslinking During Polymerization. Monomer crosslinking polymerization is one of most common particle gel synthesis methods in which free radical polymerization is initiated with the presence of crosslinkers. In this process, polymerization kinetics can be manipulated by changing reaction conditions (temperature, pH and thereof), types even amount of initiator, chelate, chain transfer agent, and other additives. Cationic, anionic, betaine or non-ionic monomers can be used in polymerization.

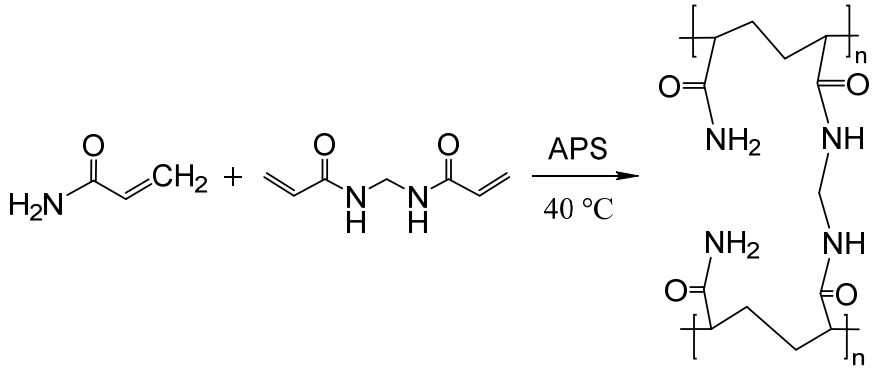

Figure 2.1. Crosslinking during the polymerization of AM.

Representative cationic monomers include dimethylaminoethyl acrylate methyl chloride quaternary salt, dimethylaminoethylmethacrylate methyl chloride quaternary salt and diallyl dimethyl ammonium chloride. Preferred anionic monomers include 2-acrylamide-2-methyl propane sulfonic (AMPS) acid sodium salt, vinyl sulfonic acid sodium salt, and styrene sulfonic acid sodium salt. Representative betaine monomers (monomers containing cationically and anionically charged functionality in equal proportions) include N,N-dimethyl-Nmethacryloyloxyethyl-N-(3-sulfopropyl)-ammonium betaine, N-(4-sulfobutyl)-Nmethyldiallylamine ammomum betaine (MDABS), and N,N-diallyl-N-methyl-N-(2- sulfoethyl) ammonium betaine. Preferred

nonionic monomers are acrylamide (AM), N-methylacrylamide, N,N-dimethylacrylamide (DMA), and methacrylamide (MAM).

The main crosslinking agent is an ethylenically unsaturated monomer containing at least two sites of ethylenic unsaturation such as methylene bisacrylamide (MBA), diallylamine, triallylamine, divinyl sulfone, and diethylene glycol diallyl ether. Varieties of initiators can be used to generate radicals that initiate polymerizations. Radicals may be generated by thermal or ambient redox conditions, meanwhile decomposition rates for some initiators vary with pH and the presence of amines. The most common classes of initiators are persulfates system such as ammonium persulfate (APS), redox system and thermal-decomposition system which involved peroxide and azo compounds.

2.2.2. Crosslinking Among Polymer Chain. Water-soluble polymers such as polyacrylamide (PAM), poly(vinylalcohol) (PVA), polyacrylate and their derivations can form gels through chemical and irradiation crosslinking [44].The chemical crosslinking reaction is the most common synthesis route for water-soluble gel.

The key in chemical crosslinking reaction is what type of bonding or association can be formed between crosslinker and polymer, which also impacts significantly on gel performance. The representative crosslinkers include multivalent metal ions and organic crosslinkers. Accordingly, two types of chemical crosslinking reactions were presented as follows; they are covalent crosslinking conducted by organic crosslinkers and ionic crosslinking accomplished via ionic crosslinkers. Here, the most commonly applied water-soluble polymer, partially hydrolyzed polyacrylamide (HPAM), was employed as the example.

2.2.2.1 Covalent crosslinking. The amido group in HPAM can react with formaldehyde and similar chemicals by condensation crosslinking as shown in Figure 2.2. In order to obtain a high strength gel, low molecular weight phenolic resin is usually used as a crosslinking agent instead of formaldehyde.

Considering the toxicity of formaldehyde, an alternative cross-linker is a type of polyamine such as polyethyleneimine (PEI). Figure 2.3 illustrated transamination reaction between HPAM or polyacrylamide/ t-butyl acrylate (PAtBA) and PEI. X is the branched backbone of the PEI. The nitrogen atoms are either primary or secondary amines.

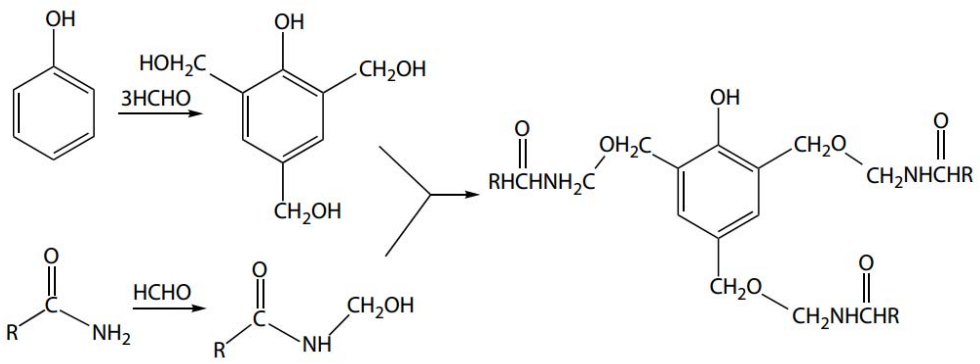

Figure 2.2. Covalent bonding formed by HPAM and phenol-formaldehyde.

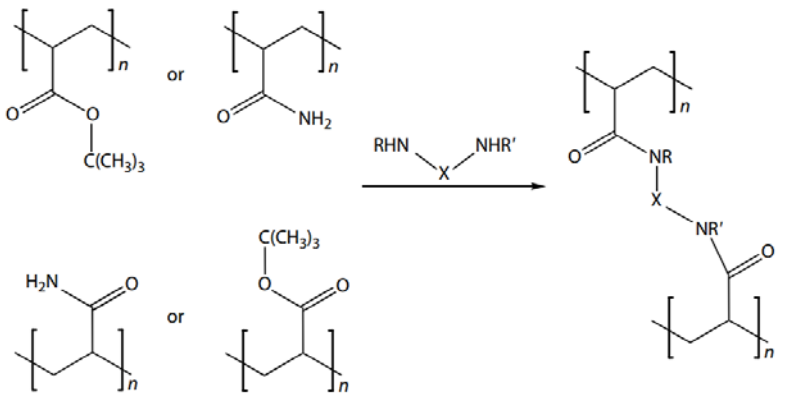

Figure 2.3. Crosslinking of HPAM or PAtBA with PEI.

Due to the amide cross-linking, gels prepared with HPAM and PEI were significantly stronger than those prepared with the Cr(III) acetate cross-linker for the same HPAM concentrations. Since PEI crosslinked HPAM gel proposed by Hardy in 1999, a number of work have reported its (or PEI crosslinked PAtBA gel's) robust performance in high temperature. PEI and PAtBA based gels were stable in the laboratory at 156°C (313°F) over months.

2.2.2.2 Ionic crosslinking. The divalent or multi-valent metal ions can form ionic bonding with HPAM. Chromium(VI), such as in dichromate ions, can be used as a crosslinker precursor that is reduced to a Cr(III) crosslinker by a reducing agent. This

system was much used in the early days of water shut-off treatments. However, this system does not give sufficient control over the gelation time. The most common metal ion cross-linkers to have been investigated are chromium(III), titanium(IV), aluminum(III), and zirconium(IV) ions. Al(III) ions as a crosslinker are rarely used because the crosslinking reaction cannot be controlled or delayed as well as other systems. A study on Al(III) cross-linked polyacrylamide gel, also known as CDG, indicated that there are two types of crosslinking reactions. One is the intramolecular crosslinking reaction that takes place in different chains of the same polymer molecule, and the other is the intermolecular crosslinking reaction that takes place among different polymer molecules. The higher the temperature, the easier the intramolecular crosslinked polymer forms.

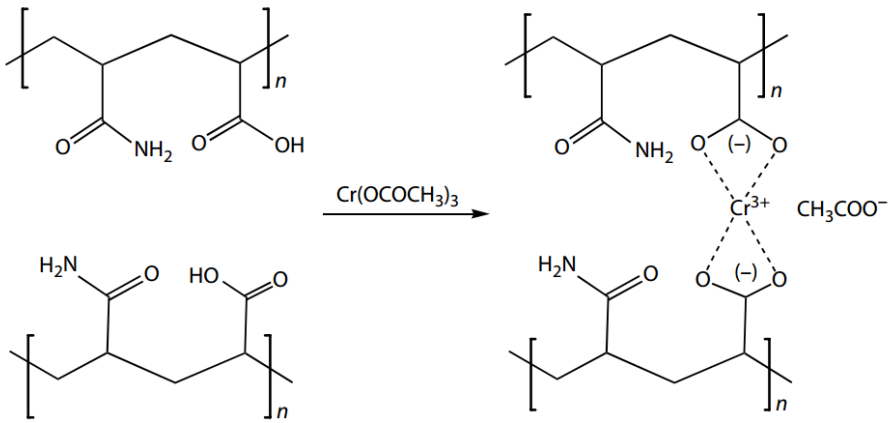

Figure 2.4. Crosslinking of HPAM with Cr(III) acetate.

To gain the control over gelation times and obtain deeper penetration of the gel, carboxylate salts of Cr(III) are used. An early and today much-used system is HPAM and Cr(III) acetate (Figure 2.4). Besides Cr(III), Zr(IV) is another commonly used metal cation cross-linker, for example Zr(IV) lactate has been deployed. Nevertheless the gel system with ionic crosslinker are widely implemented, it also has been demonstrated that the crosslinking process is prone to be impacted by multiple factors which has

constrained its application in the formation under harsh conditions of high temperature and high salinity.

2.3. LIMITATION OF CONVENTIONAL HYDROGELS

Although conventional hydrogels have been widely adopted, it is still found addressing conformance problem with the state of art has become more and more challenging. Due to the intensive environmental sensitivity, poor mechanical integrity, severe syneresis and even degradation, conventional hydrogels were not that applicable in some formations with formidable conditions such as high temperature and high salinity Hydrogels based on crosslinked polyacrylamide (PAM) were also observed unfavorable extrusions in some voids space conduits (VSC) and streaks in which the inferior stiffness and toughness of conventional gel may account for [39].

In order to propose new solutions for those defects and inspire the development of hydrogels for EOR applications, we present this work with preliminary investigations of novel technologies regrading hydrogel robustness. We expect the following modification technologies will facilitate the designing of hydrogels accommodating more diverse conditions.

2.4. ROBUST HYDROGEL WITH SUPERIOR STIFFNESS AND TOUGHNESS

In this section, three novel technologies, 1) flexibly crosslinked hydrogel, 2) nanocomposite gel and 3) double network hydrogel, were introduced respectively.

2.4.1. Flexibly Crosslinked Hydrogel. A novel type of tough hydrogel based on sliding crosslinks was introduced by Okumura and Ito in 2001[1]. These hydrogels were referred to as ‘topological gels’ (TP gels) or slip-link (or slide ring) gels, in which a number of cyclic molecules are threaded onto a linear polymer chain and then trapped by placing bulky capping groups at the two ends of the chain.

Some of the cyclics are then fused together to form mobile cross-links. In the case of two fused cyclics, the result is a figure-eight structure:∞. These cross-links are called slide rings which act like pulleys (pulley effect) for the chains threading through them. The structure is illustrated schematically in Fig. 2.5 The sliding motions are thought to equalize network stresses, cooperatively. This renders the gels unusual mechanical

properties, in particular very high extensibility and swelling ratio (~400) [1]. Indeed, tensile testing of slip-link gels illustrate that they can show very high elongations at break in excess of 1000 % [1]. An example of a rotaxane used in these studies has a flexible polymer as the linear chain and α–cyclodextrin (α–CD) units as the rings. In addition to studies of mechanical properties and swelling, the structures of these materials and their deformation mechanism have been characterized by small-angle neutron scattering (SANS) and small-angle X-ray scattering (SAXS) [2]. Recently, this modification technology has attracted increasing attention for both practical application and theoretical study.

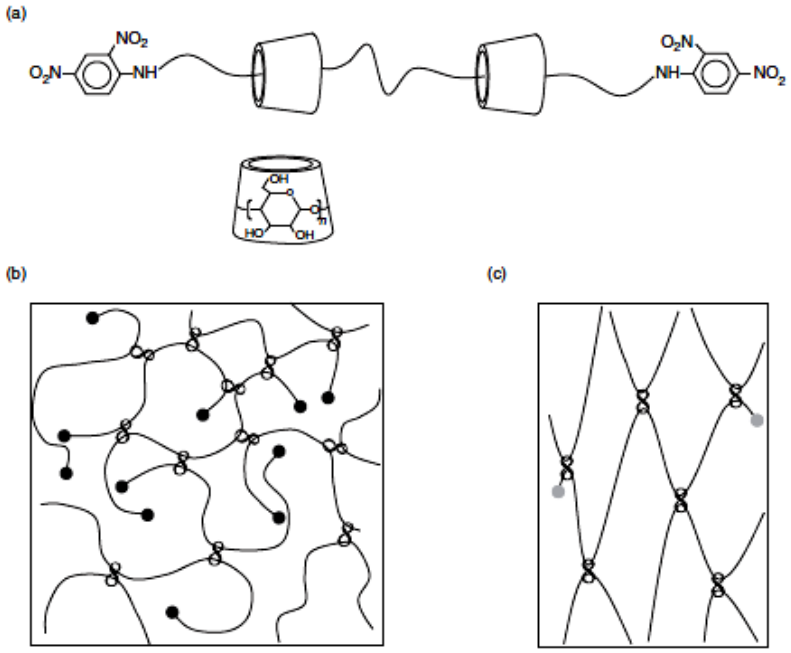

Figure 2.5. Schematic drawing of polyrotaxane.

So far, various polyrotaxanes have been investigated as new building blocks to construct microstructures as well as to realize novel functions. In these works, many types of cyclic compounds have been extensively used to construct rotaxanes and

catenanes, and the cyclic component for polyrotaxanes included crown ethers, cyclophane, calixarenes, CDs, cucurbiturils, and cyclobis (paraquat-p-phenylene)[3].

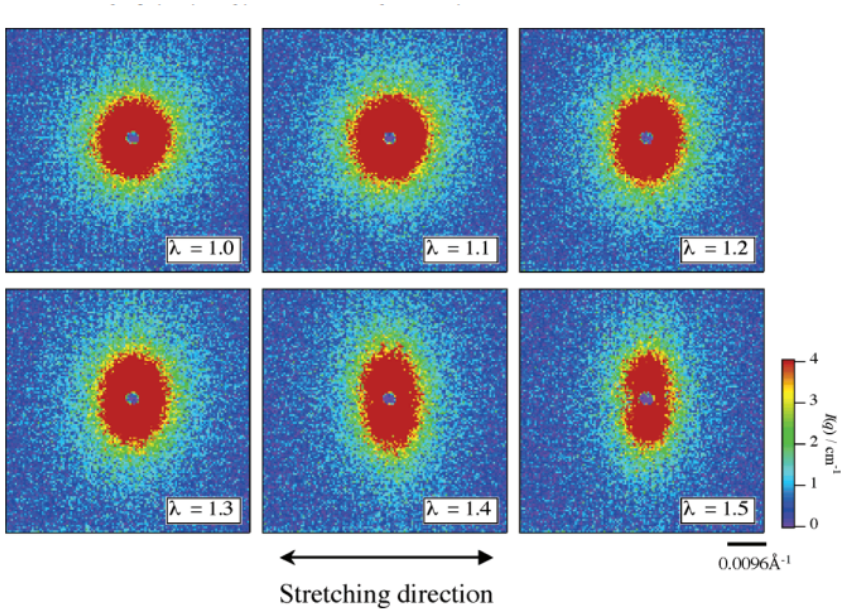

Figure 2.6. SANS patterns of slide ring gel with various stretching ratios λ.

Based on different microstructures, these polyrotaxanes can be classified as main chain polyrotaxanes and side chain polyrotaxanes (Figure 2.6). Meanwhile, they can also be cataloged as polyrotaxanes or poly*pseudo*rotaxanes due to their different synthetic approaches (Figure 2.7). To be noted, poly*pseudo*rotaxanes feature with no bulky groups blocked at the end of the polymer chain. Attributed to its unique polymeric architecture, polyrotaxanes or polypseudorotaxanes comprised of cyclodextrin especially β-cyclodextrin has been found beneficial for self-assembled formation with some guest molecules [4].Provided this property, petro-chemistry researchers committed to incorporate it with conventional chemical EOR technology.

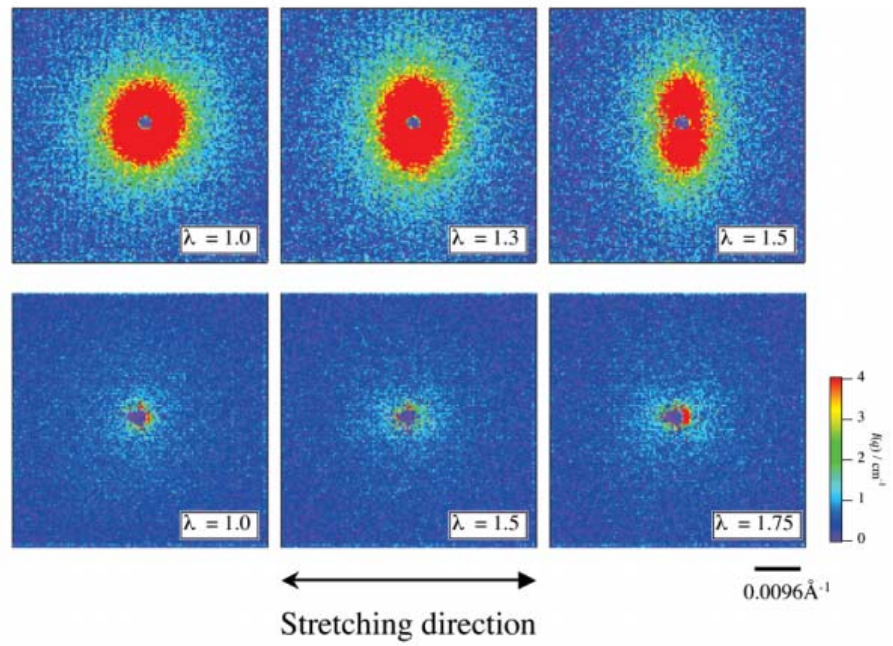

Figure 2.7. SANS patterns of slide ring gels with different CD concentrations.

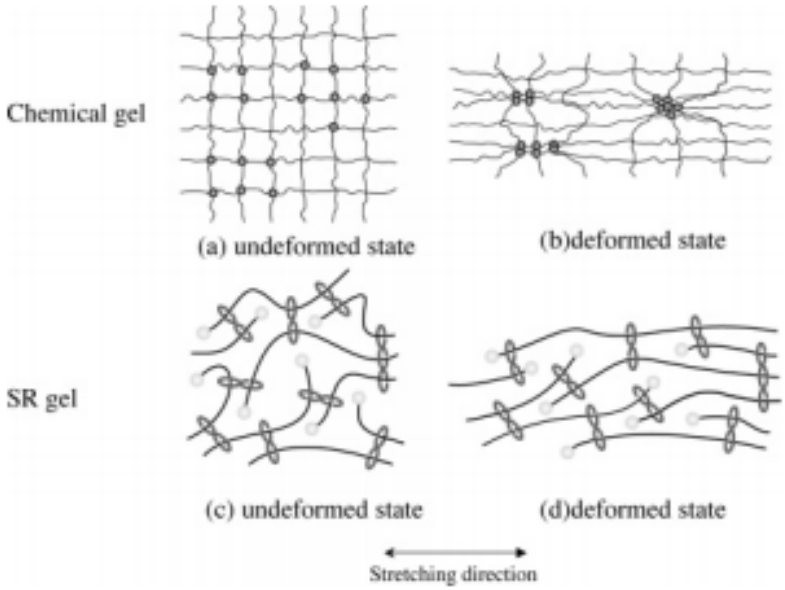

Figure 2.8. Comparison between chemically crosslinked gel and slide ring (SR) gel.

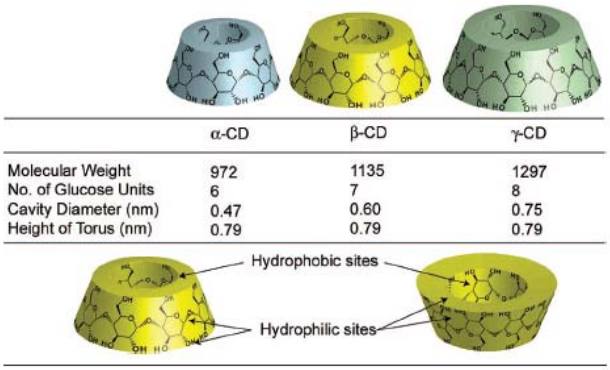

Figure 2.9. Chemical structures and properties of cyclodextrins (CDs).

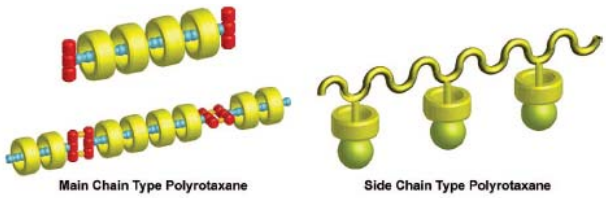

Figure 2.10. Architectures of main chain and side chain types of polyrotaxane.

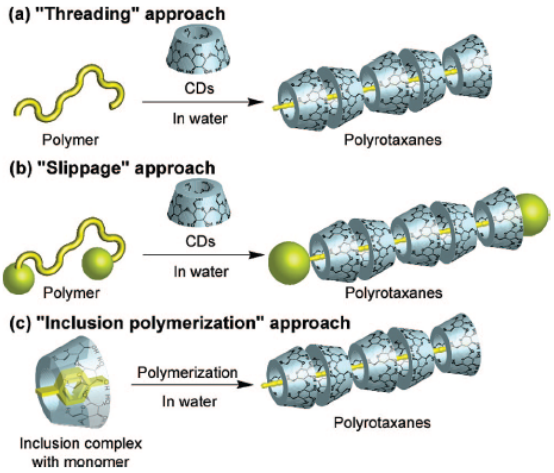

Figure 2.11. Schematic illustration of different polyrotaxane synthetic approaches.

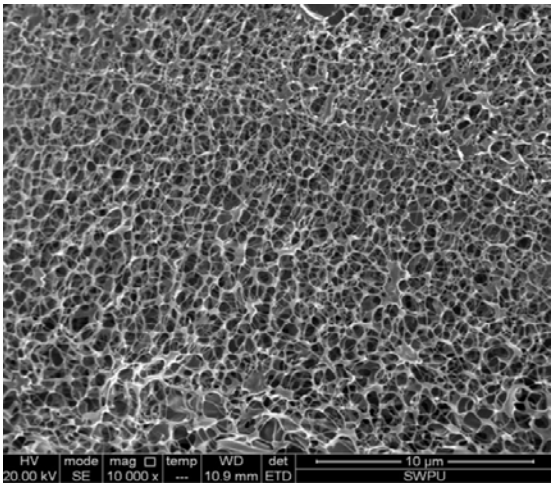

Figure 2.12. SEM image of supramolecular assembly.

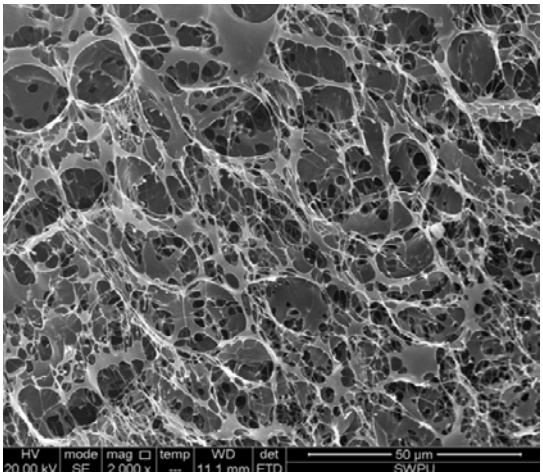

Figure 2.13. SEM image of HPAM modified by β-CD.

To the best of our knowledge, all of these researches focused on the incorporation of polymeric materials (hydrolyzed polyacrylamide--HPAM, xanthan gum--XG and et.) used for polymer flooding with β-CD or β-CD derivation. Most of these researches aimed at that β-CD or β-CD derivation would be able to enhance the performance of polymeric materials via its binding ability functioning like hydrophobicly associated polyacrylamide (HAPAM). In spite of that rotaxanes make-up polymer is getting increasing attraction, contrarily, crossliked TP gels designed for EOR applications have been barely

investigated. The application of β-CD in EOR process was first reported by Kjøniksen et al, nevertheless β-CD merely post added complex agent [5]. Liu et al investigated β-CD combined with a series of copolymer including various allyl monomers [6] and further synthesized similar polymer stabilized with clay [7]. Zou et al reported the performance of cationic β-CD inclusion complex [8][9][10]. Recently, Wei et al studied the performance of commonly used HPAM, XG and even HAPAM modified by β-CD [11][12][13]. Moreover, they also evaluated the effect of surfactant encompassing β-CD made-up polymer [14][15].

2.4.2. Nanocomposite Gel. The most extensively reported Nanocomposite (NC) hydrogels are those involving exfoliated clay nanoparticles, as first introduced and extensively studied by Haraguchi, the pioneer of NC gels [19]. Some of the NC hydrogels exhibited exceptional mechanical properties especially high elongation at break (typically 1000 %) and are commercially attractive because of their simple and fast preparing routes. NC hydrogels are formed by dispersing exfoliated clays in a monomer solution followed by *in-situ* free radical polymerization (Fig. 1.10) [19]. Significantly, organic crosslinking agent is not necessarily used and yet insoluble gel materials are formed. The crosslinking is considered to be due to stable, that is electrostatic, adsorption of the polymer onto the clay surface, with a non-covalent attachment [21]. Therefore, this kind of *physical crosslinking* is accounting for the superior performance compared with chemical crosslinked hydrogel. In fact, for an individual polymer chains, it can adsorb to a single clay nanoparticle multiple times and to many clay particles. The properties of the NC gels can also be impacted by the concentration of clay and monomer in the pre-gel dispersion. The modulus and breaking strength of the NC gels can be promoted via either increasing clay content or increasing polymer content. Over a wide range of clay contents, the elongation at break for these NC gels was at least 1000 %.

The type of clay used is also important as is the nature of the polymer [20]. To be noted that it has been indicated that NC gels cannot be achieved through simply mixing exfoliated clay with polymer solutions [22], instead, Haraguchi suggested that the adsorption of initiator to the clay surface and the subsequent polymerization is an important part of forming a tough gel [23]. It may also be possible that a particularly high molecular weight polymer is required to generate high toughness in these physically

cross-linked gels. In such cases it would be practically difficult to effectively disperse clay nanoparticles in a solution of very high molecular weight polymer. The stress-strain curves and the high extensibilities effectively illustrated their overall robustness. The large elongations measured for these gel systems suggested the absence of short strand lengths for polymer chains that connect adjacent clay particles, or, that the absorbed regions are mobile. One study demonstrated that when clay and chemical crosslinker were used together, the resulting hydrogel was brittle and exhibited low strength, similar to the gel produced with the chemical crosslinker alone. It is presumed that the chemical crosslinker introduces some degree of heterogeneity into network strand lengths then leads to localized premature failure. In contrast, recent work reported by Creton et al. described chemically-cross-linked poly(dimethylacrylamide) gels formed in the presence of silica nanoparticles and found that the toughness increased with the addition of more silica. The toughness enhancement in this case was attributed to dissipative mechanisms arising from the physical bonding between the adsorbed polymer chains on the silica particles. NC clay-based hydrogels have been shown to be significantly viscoelastic, which provides some clues as to the origin of their high toughness. Particularly at high clay contents, the load-unload curves of NC gels (after loading to 900 % strain) are hysteretic and show considerable non-recoverable strains. Re-loading of these pre-strained NC gels gives a higher modulus and strength. NC gels also exhibit nonrecoverable creep when loads less than the yield stress were applied for considerable time. The viscoelastic behaviour of these gels has been attributed to the desorption/readsorption of polymer to and from the clay surface. The clay platelets align parallel to the stretching direction as would occur in viscous flow of the surrounding polymer. During stretching, the polymer chains peel off the clay platelets, allowing for the high extensibility of the gels. These processes are similar to those occurring in carbon black-reinforced rubbers where detachment and reattachment of polymer chains to the filler surface contribute to the high fatigue resistance. It is not known at this stage whether the NC gel toughness is affected by crack speed, as would be expected if viscoelastic dissipation mechanisms were active in these materials. The ability of NC gels to show very large elongations appears to be related to the particular nature of the physical crosslinking between the polymer and the clay platelets and the high molecular

weight of the polymer. These features allow the three-dimensional network structure to be re-organized, but essentially stay intact and load-bearing, during high extensions. Each clay particle is connected to multiple polymer strands. Thus, if one strand peels off a clay particle, there are multiple neighbouring strands that can support the increased load without crack initiation. Any one chain probably has multiple attachments, separated by short loops, to a given clay particle. The multiple attachments allow the chain to detach in stages, releasing length. The bond energy of the physical adsorption of the polymer to the clay particle is similar to kT, and hence at room temperature the attachments are not permanent. If molecular weights are sufficiently high, then each polymer molecule can interact with multiple clay particles.

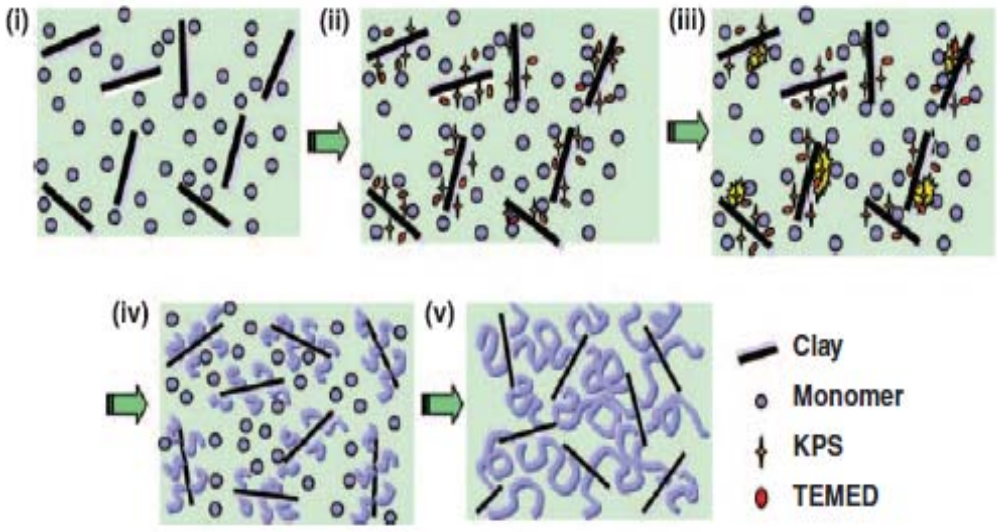

Figure 2.14. Schematic representations of the model structures.

A detached chain can re-attach to the same or another clay particle. The probability of re-attachment is increased with an increasing polymer molecular weight. The process of chain detachment and re-attachment to clay particles implies that the crosslinks undergo considerable fluctuations in space, and, as such the macroscopic strain can be much higher than the strain in a given network strand. In contrast, covalently

bonded networks are permanently damaged when a strand fractures, because the covalent bonds do not re-join.

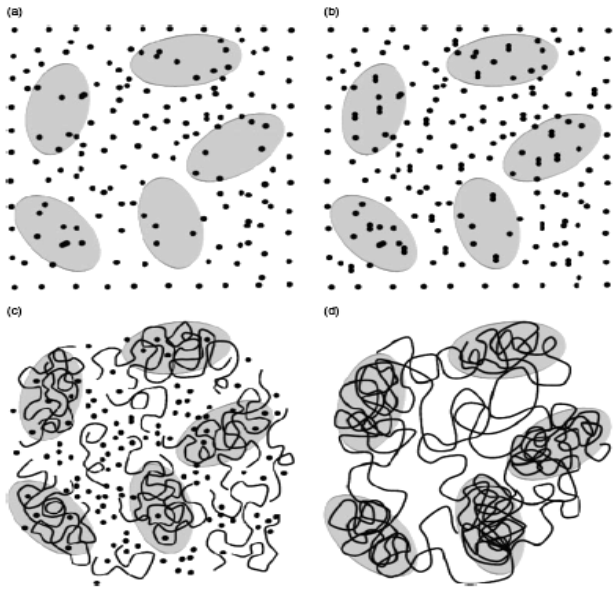

Figure 2.15. Illustration of the preparation process and structure of nanocomposite gels.

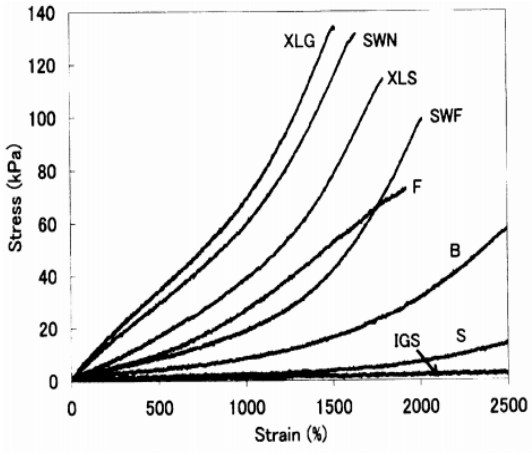

Figure 2.16. Stress–strain curves of D-NC gels.

2.4.3. Double Network Hydrogel. Double network (DN) hydrogels are to date the toughest synthetic hydrogels. These materials were introduced by Gong et al. in 2003 [16], with spectacularly high compression strength in comparison to the conventional 'single network' system. For example, a DN formed by poly2-Acrylamide-2-methylpropanesulfonic acid (PAMPS) and polyacrylamide (PAM) revealed a compression strength of 17 MPa, while the PAMPS single network failed at just 0.4 MPa and the PAM single network had a compressive strength of just 0.8 MPa. DN hydrogels consist of two independent networks and sequentially prepared. The first network to be prepared is soaked in a solution containing the monomer of the other (referred to as the second network), which is subsequently polymerized. DN hydrogels display remarkable robustness in tension, as do tough thermoplastics and some metals. Some DN hydrogels have been evaluated using fracture tests (like the trouser tear test) to give fracture energy measurements. To achieve high toughness, a high molar ratio of the second network to the first (typically greater than 10 times) and a very low degree of crosslinking in the second network are required. The commonly used synthesis methods ensure that there is usually some degree of chemical bonding between the two networks as active double bonds remaining in the first network from half-reacted bi-functional crosslinking agents can participate in the second network polymerization. In the case of truly independent PAMPS-PAM, DN gels the fracture strength of samples with linear PAM chains as the second network were shown to be much lower than those with a critical amount of crosslinking (i.e. those prepared with ,0.01 mol % bifunctional crosslinker). Although the largest compressive strength for a highly swollen hydrogel was obtained when the first network was a rigid polyelectrolyte and the second network was a flexible neutral polymer, there are many different DN hydrogel systems reported in the literature with all displaying enhanced toughness relative to the equivalent single networks.

The mechanism of toughening and strength enhancement in DN hyrdogels appears to be related to the stabilization of micro-cracks that form in the first network. Okumura, Brown and Tanaka have independently proposed phenomenological models to explain the toughness of DN gels. The Brown model considers that the gel toughness is increased by the DN topology, allowing for a 'damage zone' to develop around the crack tip. The damage consists of fractured strands of the first network. As in the Lake-Thomas

description of elastomer toughening, the fracture of these network strands absorbs energy. In conventional single networks, there are comparatively few strand fractures needed to generate a series of micro-cracks that coalesce into a growing macro-crack. Micro-cracks also initiate within the first network of the DN hydrogels, since the first network has a higher degree of crosslinking, is heterogeneous, and is already stretched due to swelling in the second network's monomer stage of the gel preparation process. In contrast to single network hydrogels, the micro-cracks that form in the first network of a DN hydrogel are bridged by the loose strands of the second network, stabilizing these micro-cracks so that they do not readily coalesce and propagate. Further micro-cracks can then be formed thereby generating a damage zone of up to several hundred microns in thickness. The enhanced toughness of DN hydrogels is then directly related to the considerably increased number of strand fractures needed before crack propagation occurs in DN gels in comparison to that required in the single network gel.

Recent studies have provided direct support for the 'damage zone' model from various experimental techniques. Microscopic images of the crack tip in a PAMPS-PAM DN gel clearly show a damaged area developed around the crack tip as presented. It was shown that the size of this damaged zone (h, 100–800 mm) has a linear relation with the recorded fracture energy in the tearing test. Second, it has been observed that tensile loading-unloading studies of DN hydrogels demonstrate a large hysteresis during the first load-unload cycle that is mostly absent in subsequent load-unload cycles (to the same maximum extension). Second (and subsequent) cycles also show a reduced shear modulus compared with that seen during the first cycle. These results can be interpreted as being due to irreversible scission of short network strands during the first loading cycle. Other experimental results show that the fracture energy of DN gels hardly depends on crack velocity, which indicates that the high fracture energy of DN gels cannot be explained by viscoelastic dissipation processes, as these would be very time-dependent. While many details of the toughening mechanism still need to be resolved, the general picture of energy dissipation occurring throughout a significant volume in DN gels appears consistent with the experimental observations. The necking phenomenon observed for some DN gels is striking. For a neck to form, the implication is that the damaged zone passes through the cross-sectional area as one continuous zone. Hence, the

second network is taking on the majority of the load. This unusually strong polymer network can be explained by one of two possibilities: the second network is less heterogeneous than if synthesized alone and/or portions of the first network remain and act as slip links.

Interestingly, the toughness enhancement of DN gels show some parallels to the improved strength previously reported for ‘bimodal elastomers’. These elastomers have a bimodal distribution in strand lengths, with a molar ratio of short chains to long chains in the range of 90–95 %. The toughness of bimodal elastomers was also independent of strain rate and, hence, not due to viscoelastic processes. The key difference between DN hydrogels and bimodal elastomers is that the DN hydrogels are formed with a heterogeneous crosslink distribution in the first network, while the elastomers have defined chain length. The short chains often employed in bimodal elastomers are so short that the swelling ratio would be limited in a swollen state. Further evaluation of the fracture mechanisms operating in bimodal network elastomers may shed further light on the toughening processes occurring in DN gels.

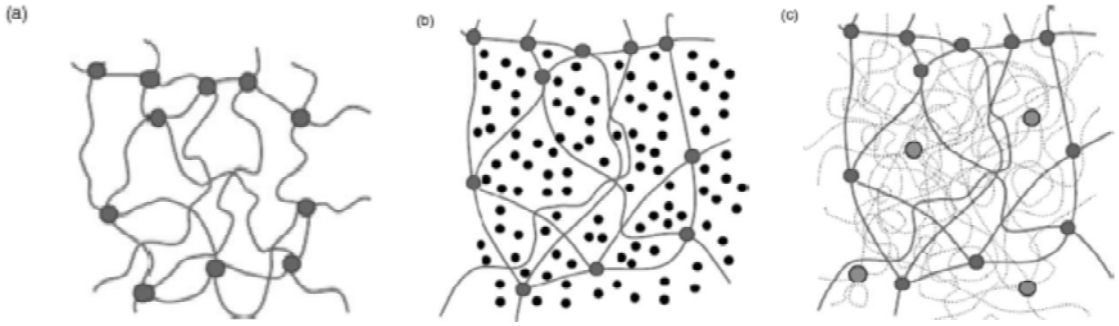

Figure 2.17. Schematic diagram illustrating the two-step method used to make DN gels.

3. DEVELOPMENT AND OPTIMIZATION OF STARCH-GRAFTING-POLYACRYLAMIDE NANOCOMPOSITE HYDROGEL FOR CONFORMANCE CONTROL

3.1. EXPERIMENTAL

Experimental study was initiated from the preparation of particle; followed by the optimization and evaluation of SAC; and finalized with a series of characterization.

3.1.1. Materials and Preparation. The monomer, acrylamide (AM, 98%), was bought from Alfa Aesar. The crosslinker, N,N'-methylene bisacrylamide (MBA, 99%), and some other additives such as soluble starch (Certified ACS), ethylenediaminetetraacetic acid disodium salt (EDTA-2Na, 99%), urea (NH_2CONH_2, USP) were purchased from Sigma-Aldrich. The initiator, ammonium persulfate ($(NH_4)_2S_2O_8$, Certified ACS), sodium sulfite (Na_2SO_3, Certified ACS), sodium hydroxide (NaOH, Certified ACS), sodium chloride (NaCl, Certified ACS), were supplied by Fisher Chemical. The nanoclay used in this work belonged to a type of sodium-montmorillonoid (Na-MMT) provided by Wyoming Bentonite ^{SM} with a trade name of Hydrogel®. Reversed Osmotic (RO) water was laboratory purified.

Starch is a kind of carbohydrate, obtained by photosynthesis of plants. It has two different structures, amylose and amylopectin, which have been discussed and reviewed by many authors. Amylose (Figure 3.1) is a relatively long, linear α-glucan containing around 99% (1-4)-α-linkages and around 1% (1-6)-α-linkages, while amylopectin (Figure 3.2) has a highly branched structure containing about 95% (1-4)-α-linkages and about 5% (1-6)-αlinkages.

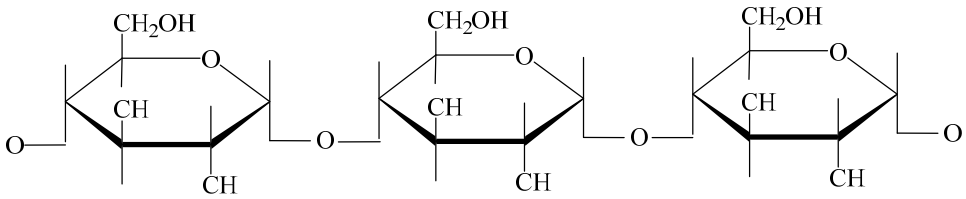

Figure 3.1. Configuration of amylose.

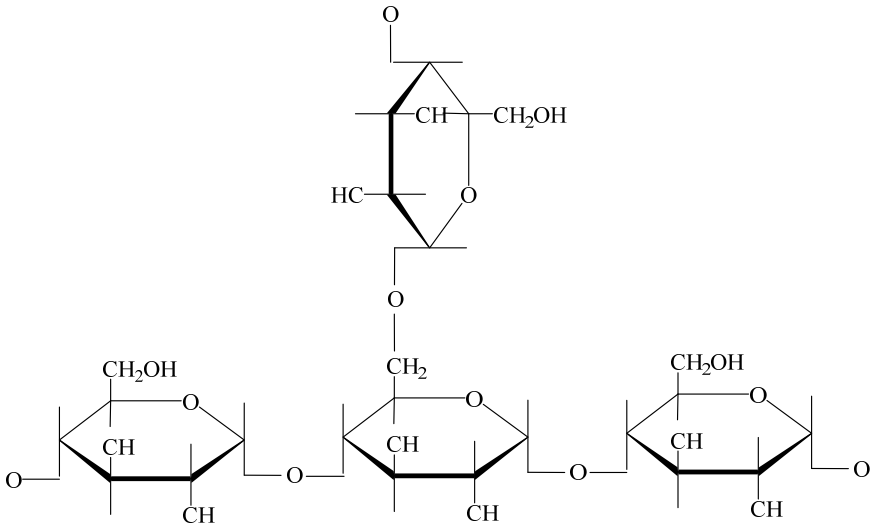

Figure 3.2. Configuration of amylopectin.

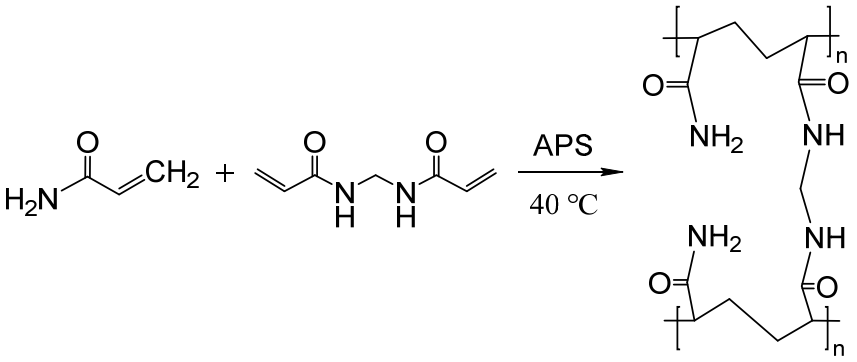

Figure 3.3. Schematic of crosslinking polymerization between acrylamide and N,N'-methylene bisacrylamide.

To present the preparation of SAC gel, the fabrication of specimen PPG6-3 was detailed as an example. First, 30.79 g AM and 2.82 g MBA solution (2 wt%) was predissolved in 30 ml RO water. This predissolution was accomplished with a magnetic stirring at room temperature (25 ℃) for 1 hour. Afterwards, 4 g MMT was slowly added into the bicomponent solution of monomer and crosslinker. A 30 minutes ultrasonic dispersing followed this. At the meantime, a suspension that consisted of 9.85 g of starch and 15 ml RO water was prepared in a 100 ml flask. In order to facilitate the gelatinization of starch, 2.93 g of NaOH solution (15 wt%) was dropped into the

suspension. As we know, starch granules are quite resistant to water penetration at low temperature (25 ℃) due to intramolecular and intermolecular hydrogen bonding. Heating in aqueous condition to weaken the strong bonding is commonly called starch gelatinization and also a typical approach to obtain starch solution. Herein our experiment, gelatinization of starch was carried out at 80 ℃ with an oil bath. In addition, a mechanical stirring had been imposed for 2 hours to achieve an adequate gelatinization. Subsequently, the flask was moved to room temperature for an ambient cooling. The mixing of clay dispersion and starch solution took place with an aid of high-speed blending. Then, a deoxide with Nitrogen was conducted for 30 mins prior to which 2.49 g APS solution (14 wt%) was dropped. Eventually, the specimen was kept in 40 ℃ oven heated for 6-8 hrs. This formed bulk gel was further dried in room temperature and cut into small pieces. Screened by the shaker, gel particles with certain size have been achieved and well-prepared for the further utilization.

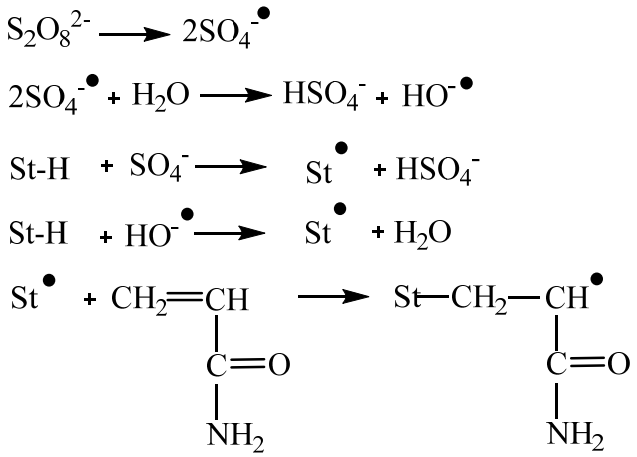

Figure 3.4. Grafting reaction between starch and acrylamide.

3.1.2. Optimization and Evaluation of SAC. As the flowchart (Figure 3.5) showing, the optimum formulation was achieved through varying the concentration of each component and investigating the effects of varied components. In optimization process, gel swelling ratio and rheology strength were two predominated parameters which were most highlighted. Eventually, the specimen with tunable swelling ratio and

gel strength was considered as optimum SAC gels and furtherly performed with more evaluations.

The optimum concentration of crosslinker, MBA, was explored at the very beginning followed by an investigation of optimum concentration of initiator. Afterwards, additives involving starch, NaOH (aq), MMT and Na_2SO_3 were studied respectively for their optimum concentrations.

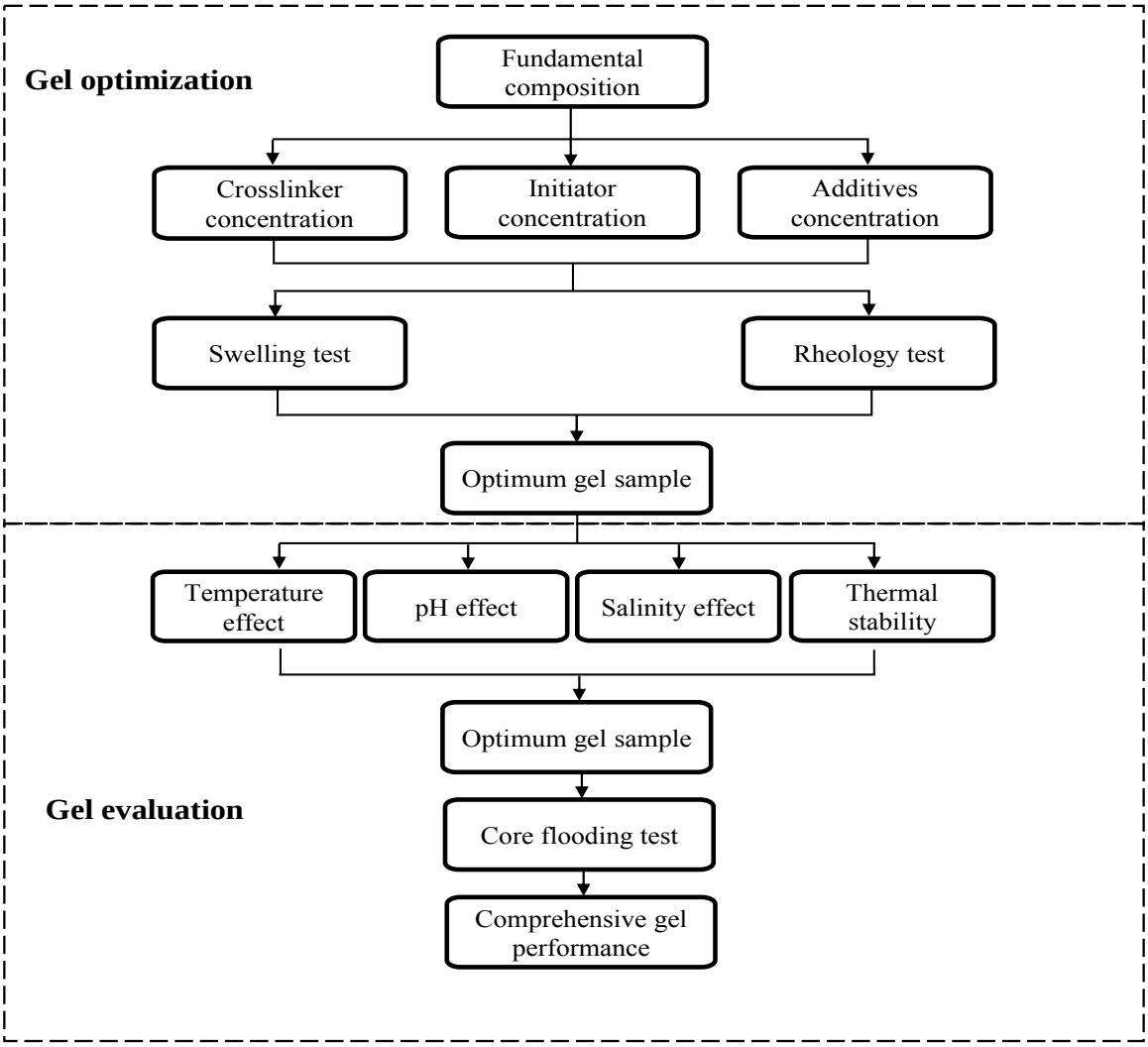

Figure 3.5. Experimental design and flowchart of gel optimization and evaluation.

3.1.2.1 Swelling test. Dried crude hydrogel was cut into particles with size of 20-30 mesh (0.60-0.85 mm). These particles were placed into conical graduate tube with volumetric scale. Dry particles' volume was measured and immersed into brine with designed salt concentration for a complete expansion and then the swollen volume was measured under room temperature (25 ℃). To evaluate gel swelling behavior in aqueous with salinity, NaCl brine with different concentrations of 0 wt.%, 0.25 wt.%, 0.5 wt.%, 1 wt.%, and 2 wt.%.was prepared. The same procedure was conducted for the solutions with different pH values (2~7) which are adjusted by aqueous HCl and NaOH solution to assess the swelling performance of particles at conditions with different pHs. The following equation was used for swelling ratio calculation,

$$SR = \frac{V_a}{V_b} \tag{1}$$

in which SR represented gel swelling ratio; V_a stood for gel volume after swelling; V_b was gel volume before swelling.

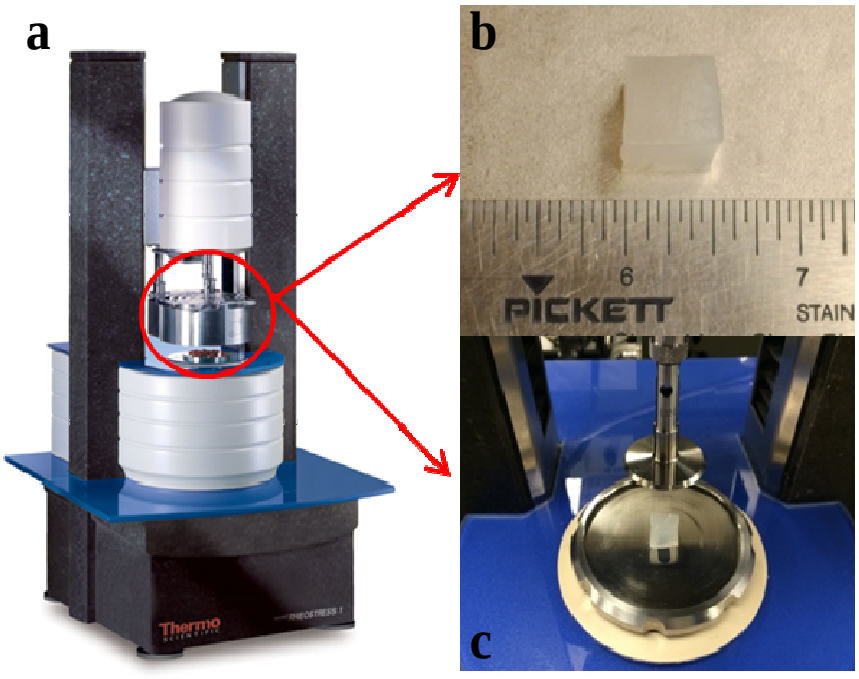

Figure 3.6. (a) HAAKE Rheoscope1 rheometer, (b) gel disc prepared for rheology testing and (c) PP 35 Ti plate-plate geometry for DRM.

3.1.2.2 Rheology property. The rheology properties of SAC were investigated using HAAKE Rheoscope1 rheometer (Germany) with plate-plate geometry (PP35 Ti). Besides, all sets of rheological measurements were carried out in ambient (25 ℃) with an implement of solvent trap to prevent vaporization. The testing specimen were prepared by crafting the swollen bulk gel into a cubic gel disc sizing of 12 mm* 12 mm*3 mm.

The approach, dynamic rheological measurement (DRM), was exploited in this study, in which a stress and frequency dependent, oscillatory shearing was imposed on gel specimen. In DRM, amplitude sweep is the most common method involving stress sweep and frequency sweep tests. The dynamic stress sweep was carried out with a stress varied from 0.1 pa to 10000 pa, and a fixed frequency of 6.28 rad-1 (1 Hz). After this process, frequency sweep was conducted with an oscillatory frequency ranged from 0.01 to 100 rad-1 (0.00159-15.9Hz) and a constant stress determined by stress sweep. Finally, the storage modulus (G') and loss modulus (G'') of each specimen were achieved for the further comparison.

3.1.2.3 Core flooding test. To investigate optimum gel performance in fracture aperture, three sets of core flooding tests were carried out with Berea sandstone cores which differed in permeabilities. The fractured core preparation procedure was as follows:

(1) The sandstone cores were oven dried at 120℃ for 24 hrs to remove the residual water. Then, a series of basic parameters including length (L), diameter (D), and dry weight (M) were measured in ambient.

(2) A specific core would be vacuumed for at least 4 hrs and then saturated with 1 wt% NaCl brine for 6 hrs. After brine saturation, a weight measurement was conducted to obtain the pore volume (PV) and porosity (φ).

(3) The core was mounted into the core holder and furtherly loaded with a constant overburden pressure of 500 psi. In order to achieve the matrix permeability (K), 1 wt% NaCl brine was injected with four different flowrates (2.0 ml/min, 3.0 ml/min, 4.0 ml/min, 5.0 ml/min), while the real-time injection pressure was recorded. Until when steady-state flow was established, the matrix permeability (K) could be calculated via Darcy's law.

(4) The core was subsequently flooded by oil which possessed a viscosity of 14.3 cp in ambient. The injection flowrate was maintained at 0.8 ml/min thus the original oil saturation (OOIP) and irreducible water saturation (Swi) could be achieved.

(5) The oil-saturated core was taken out from the core holder. A longitudinal fracture was created along the core carefully and smoothly using a band saw. On the surface of one core segment, two identical pieces of incompressible steel (125 mm*50 mm*1.2 mm) were attached with adhesive agent. Once these two segments had been assembled, the entirety simulated the fracture aperture in which the steel performed as spacers to prop the fracture. One step further, we tied the segments up using Teflon® to ensure they had been assembled firmly.

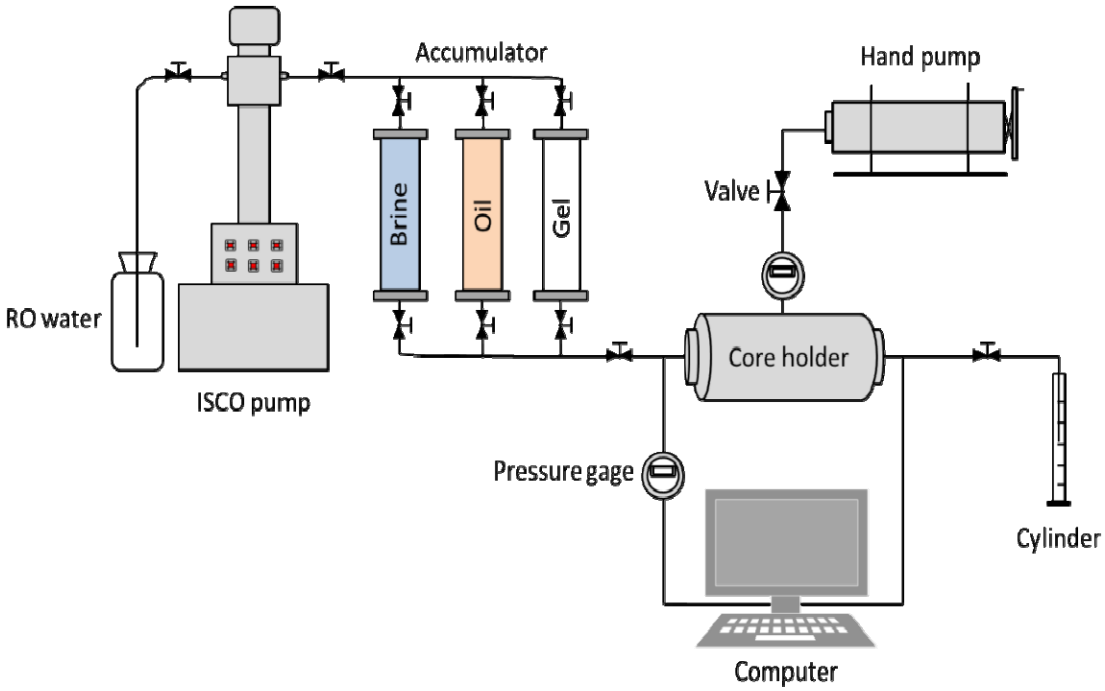

Figure 3.7. Experimental setting-up of core flooding test (I).

(6) The core with artificial fracture was again mounted into the core holder followed by a brine injection with constant flowrate (2 ml/min). This process was considered as first water flooding in which brine was injected until the water cut reached

as high as 98%. Meanwhile, the oil recovery was quantified through collecting the produced oil from outlet.

(7) Gel treatment was carried out after first water flooding. Swollen particle gels (0.48-0.8 mm) without free water had been placed in the accumulator and then injected into fracture aperture with a constant flowrate of 1 ml/min. Aiming at an effective fracture remediation, particle gels had been injected with an amount of 10 FV.

Table 3.1. Parameters of sandstone cores used in core flooding tests.

Core code	Length (mm)	Diameter (mm)	Matrix permeability (md)	Porosity (%)	Pore volume (cm^3)	Fracture volume (cm^3)
#1	124.9	50.32	18.3	16.89	49.8	7.5
#2	125.0	50.50	149.6	16.78	49.5	7.5
#3	124.8	50.34	361.0	17.25	50.7	7.5

(8) Second water flooding took place next to gel treatment. Similar to the first water flooding, brine was injected at a constant flowrate (2 ml/min) until the water cut raised up to 98%. Besides, the injection pressure was recorded meanwhile the produced oil was collected to achieve the residual resistance factor (Frr) and cumulative oil recovery.

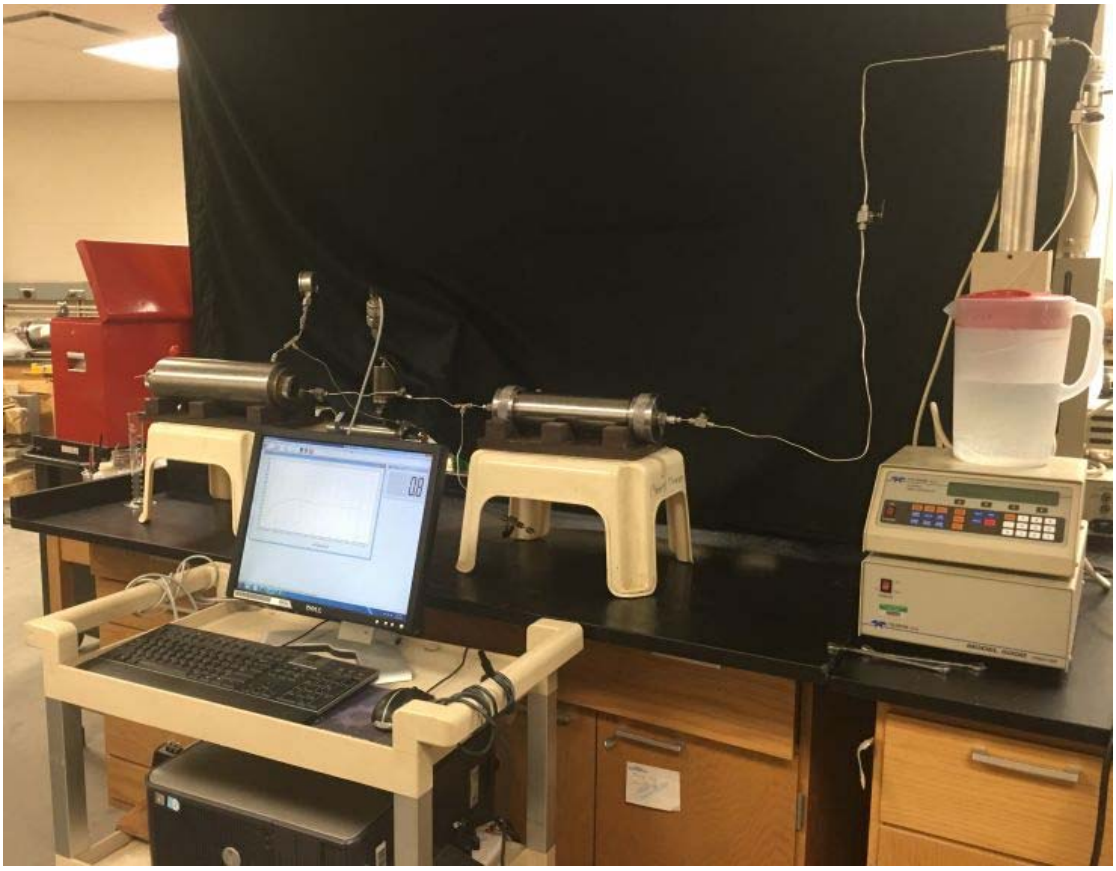

Figure 3.8. Experimental setting-up of core flooding test (II).

Figure 3.9. Sectional and longitudinal of fractured core before gel treatment.

Figure 3.10. Sectional and longitudinal of fractured core after gel treatment.

3.1.3. Characterization of SAC. FT-IR and scanning electron microscopy were utilized to characterized the component and microstructure of SAC respectively.

3.1.3.1 Fourier transform-infrared spectroscopy (FT-IR). FT-IR spectra of SAC specimen were achieved using Nexus 470 FT-IR (Thermo Electron Corp.). In order to prepare testing pellets, SAC particles were first oven dried, and then mixed with KBr at a ratio of 1:100 (wt/wt). The characteristic peaks were collected with a setting of 16 signal-averaged scans at resolution of 2 cm^{-1} in mid-IR region (4000–400 cm^{-1}) for pure KBr and for SAC-KBr mixed specimen.

3.1.3.2 Scanning electron microscopy (SEM) study. The microstructure of SAC was characterized with Hitachi S-4700 Field Emission Scanning Electron Microscope (SEM). Swelled SAC particles (0.6-0.85 mm) were first frozen with liquid nitrogen which was followed by a 12 hour freezing-dry process. Then, the dried hydrogel networks were placed on a piece of conductive tape which was attached to the stainless steel stub, and sprayed with Au/Pd nano-particles for 3 min. SEM imaging was conducted using a field emitter source via a mixed detector at 15 kV accelerating voltage, and 9.5 μA current.

3.2. RESULTS AND DISCUSSION

The results of optimization experiments were thoroughly studied and analyzed based on the swelling ratio and storage modulus of each sample. Afterwards, the evaluation conducted with core flooding test indicate the efficient plugging performance of SAC.

3.2.1. Optimization of Crosslinker Concentration. Initially, the monomer concentration and initiator (aq) concentration were maintained at 30.79 g and 2.49 g respectively. Through varying crosslinker concentration, optimum crosslinker concentration was achieved upon comparisons of swelling ratio and storage modulus.

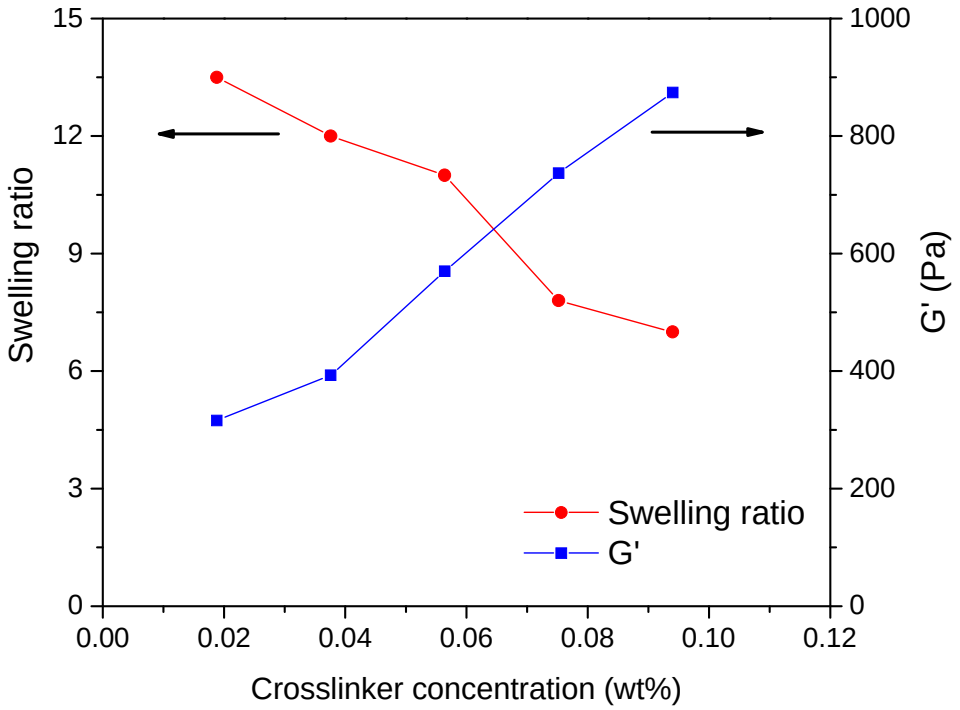

Figure 3.11. Gel swelling ratio and G' versus various crosslinker concentrations.

As displayed in Figure 3.11, storage modulus (G') was enhanced with an increasing addition of the crosslinker, MBA, meanwhile the swelling ratio decreased. According to Flory–Rehner theory, both gel strength and swelling ratio were closely related to the crosslinking density of gel network. For instance of PPG1-1 and PPG1-2,

the concentration of MBA was insufficient to establish crosslinking points and buildup rigid 3-D network. Whereas, the absence of rigid network would not interfere water diffusion, instead, the larger "pore structure" in network facilitated water retention. Although PPG1-4 and PPG1-5 characterized superior storage modulus, these two specimen were also indicated that excessive crosslinking rendered the gel unfavorably brittle.

In general, the moderate MBA amount, 2.82 g, which formulated PPG1-3 was considered an appropriated crosslinker concentration. Thus, in following study, crosslinker concentration of PPG was always kept at 2.82 g.

Table 3.2. Gel swelling ratio and G' versus various crosslinker concentrations.

Specimen	Crosslinker concentration (g)	Swelling ratio (ml/ml)	G' (Pa)
PPG1-1	0.94	13.5	316
PPG1-2	1.88	12	393
PPG1-3	2.82	11	570
PPG1-4	3.76	7.8	737
PPG1-5	4.7	7	874

3.2.2. Optimization of Initiator Concentration. Initiator concentration was of great significant for free radical polymerization, affecting polymerizing rate and polymer's molecular weight. Hence, a typical gel precursor system was used to study the initiator concentration effect: a 29.8 g monomer concentration, a 2.82 g crosslinker MBA, and a 40°C synthesis temperature in a water bath.

Figure 3.12 represented the effect of the initiator concentration on the gel's storage modulus and swelling ratio. In addition, the gelation time was also observed a

dramatic decreasing as the initiator concentration increased, due to the increased amount of initiators cleaving into more free radicals which accelerated polymerization.

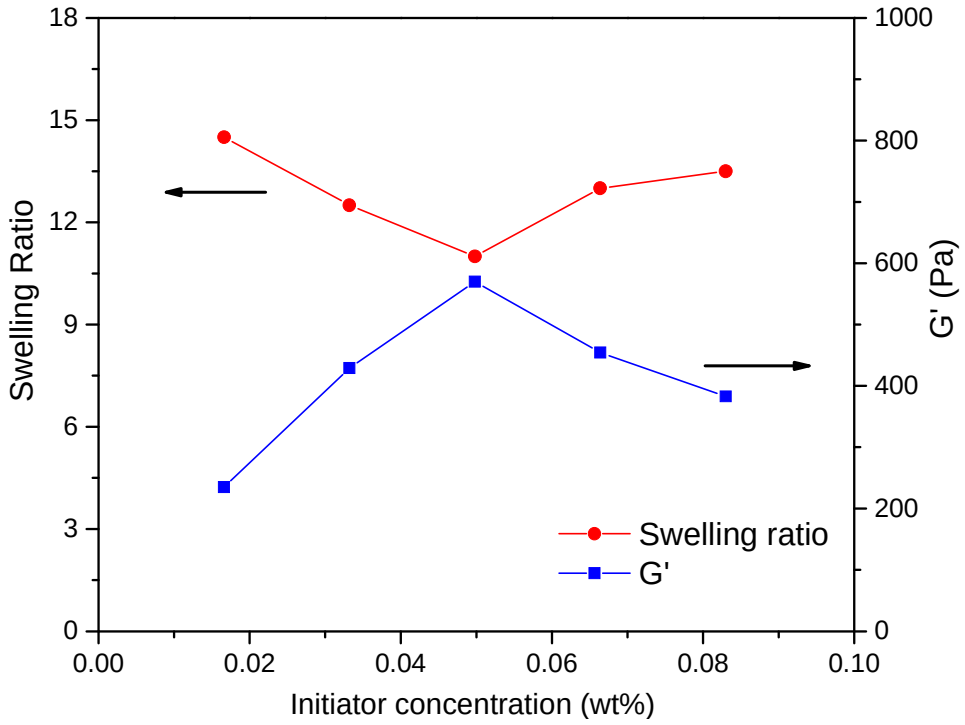

Figure 3.12. Gel swelling ratio and G' versus various initiator concentrations.

When the initiator concentration was less than 2.49 g, gel strength increased with the initiator concentration. When the initiator concentration was higher than 2.49 g, the gel strength (G') decreased. The phenomenon of gel strength first increasing and then decreasing was related to the microstructural evolution during polymerization.

Initially, the cyclization of pendant vinyls from acrylamide monomers readily form highly crosslinked microgel clusters. The crosslinking takes place in these clusters with excess crosslinkers due to its higher reactivity relative to the acrylamide monomer, while the monomers themselves initially are not associated with the chain growing process. Gradually, fewer crosslinkers are available within the individual clusters. The crosslinking reactions start at the remaining active sites in the end groups and the

peripheral pendant vinyls from the clusters, and subsequently a global gel network forms. The resulting lightly crosslinked gel network is formed by an inhomogeneous assembly of tightly crosslinked micro gel clusters. When the initiator concentration is lower than 2.49 g, the formation of microgel clusters and subsequent gel networks is dependent on the decomposition rate of the initiators. The gelation time decreased and the gel strength (G') increased as the initiator concentration increased.

Table 3.3. Gel formation time, swelling ratio and G' versus various initiator concentrations.

Specimen	Initiator concentration (g)	Gel formation time (hour)	Swelling ratio (ml/ml)	G' (Pa)
PPG2-1	0.83	8	14.5	235
PPG2-2	1.66	4	12.5	429
PPG2-3	2.49	2.5	11	570
PPG2-4	3.32	2	13	454.5
PPG2-5	4.15	1.5	13.5	383

When the initiator concentration was higher than 2.49 g, a high dosage of initiators triggered most of monomers and crosslinkers reacted during the microgel cluster formation process. When the initiator concentration is higher, fewer monomers and crosslinkers are available for interdomain crosslinking. This leads to the average polymer chain length being very low, which may have a significant impact on the gel's stability.

This is due to the formation of polymer chains so short that interdomain crosslinking cannot take place. The initiator concentration of 2.49 g may balance the formation of microgel clusters and interdomain gel networks, which could lead to the

maximum possible gel strength. At higher initiator concentrations (e.g. 3.76 g), shorter polymer chains were formed in the loose interdomain cross linking network due to the lack of monomers and cross linkers. At lower initiator concentrations (e.g. 1.88 g), much longer polymer chains were formed, which gives more elasticity to the gel network. Oxygen may start to take effect and inhibit polymerization if the reaction is too slow at low initiator concentrations. Therefore, to ensure the gel viscoelasticity and swelling ratio the recommended initiator amount is 2.49 g.

3.2.3. Optimization of Starch Concentration. Starch with varied concentration was furtherly introduced into the precursor system.

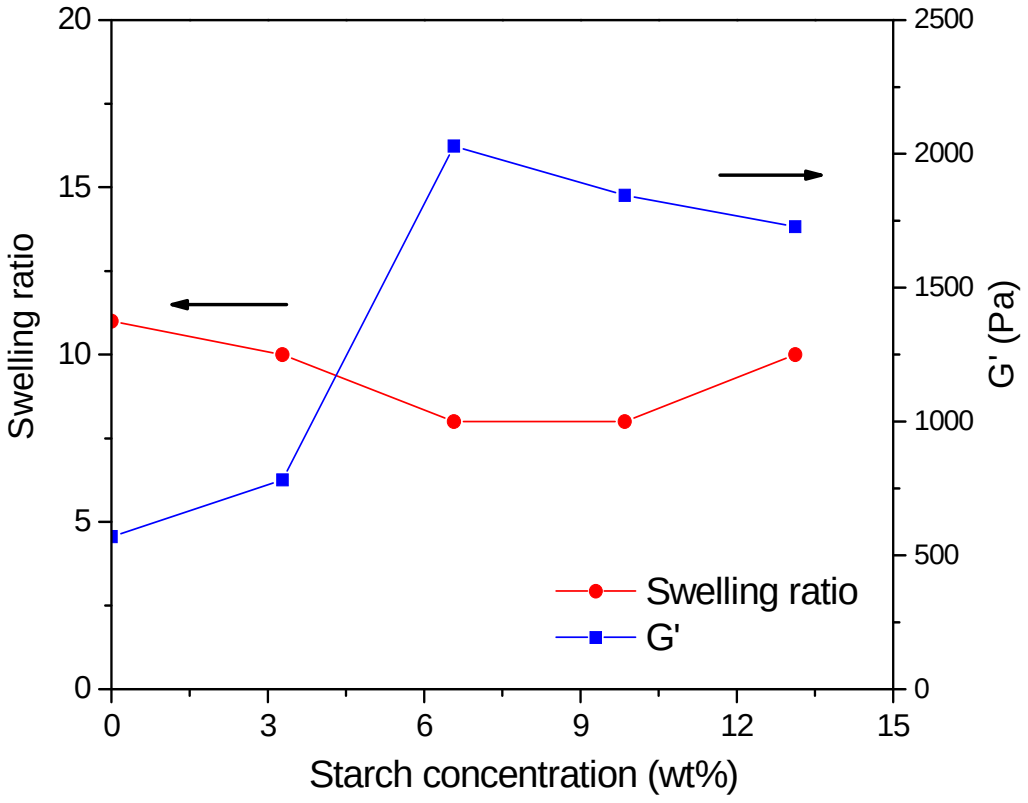

Figure 3.13. Gel swelling ratio and G' versus various starch concentrations.

Within this study, monomer concentration was kept at 29.8 g, with a crosslinker of 2.82 g and an initiator of 2.82 g. To facilitate starch gelatinization, NaOH solution was implemented at a constant ratio of starch concentration.

As shown by Figure 3.13, gel strength (G') was subjected to a rapid increase when starch concentration was relatively low (e.g. 3.28 g and 6.57 g) and then slightly decreased during which starch concentration was larger than 6.75 g.

Once the starch was grafted on the chain of PAM, an "encapsulation" configuration formed as Figure 3.14 illustrated, which was also confirmed by SEM observation. Taking advantage of this "encapsulation" configuration, the entanglement within polymer chain was thereby enhanced. It was noted that this enhanced entanglement has contributed to a strengthened viscoelasticity, namely a superior gel strength.

Whereas, an excessive addition (e.g. 13.12 g) may also render the starch molecule play a role of chain transfer agent interfering chain propagation of PAM and even brought an impact on its molecular weight. Therefore, starch concentration of 9.85 g was finalized as the optimal concentration of starch.

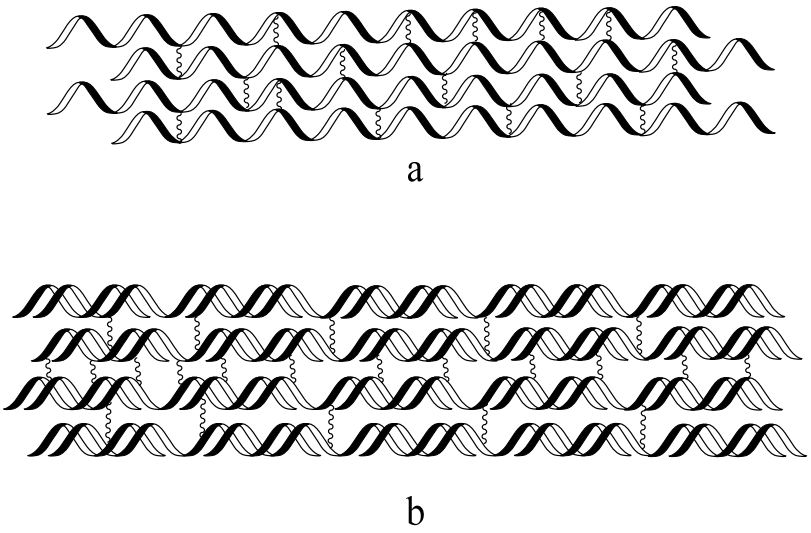

Figure 3.14. Different configurations of (a) crosslinked PAM and (b) crosslinked PAM-g-starch.

Table 3.4. Gel swelling ratio and storage modulus G' versus various starch concentrations.

Specimen	Starch concentration (g)	Swelling ratio (ml/ml)	G' (Pa)
PPG3-1	0	11	570
PPG3-2	3.28	10	782
PPG3-3	6.57	8	2029
PPG3-4	9.85	8	1845
PPG3-5	13.12	10	1728

3.2.4. Optimization of NaOH Concentration. Due to the existence of substantial hydroxyl groups (-OH) in starch chain, the intermolecular association among starch granules was considerably strong.

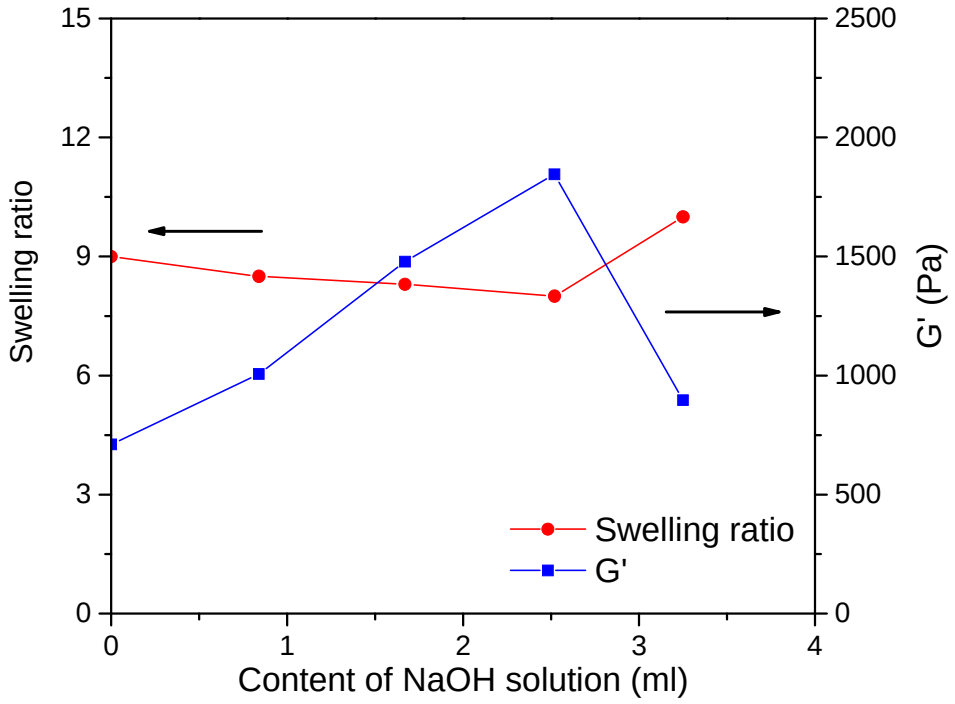

Figure 3.15. Gel swelling ratio and G' versus various NaOH (aq) concentrations.

Thus, the process of gelatinization was necessary for achieving starch solution and making starch participate in further reactions. Accordingly, a 2 hour, water bath heating was loaded for starch gelatinization. Furthermore, NaOH solutions with various concentrations were introduced into precursor system to facilitate gelatinizing starch. In this study, concentrations of starch, AM, MBA, and APS were all fixed as constant, leaving the concentration of NaOH as the single variable.

The experimental results indicated that, within the range of 0.98 g to 2.93 g, the introducing of NaOH solution functioned in improving gel strength.

At the beginning, the hydroxyl ions provided by NaOH solution performed as an efficient catalyst for the hydrolysis reaction of starch. As expected, this hydrolysis reaction accounted for the favorable disassociation of starch chains, marked that gelatinized starch would be more prone to participating in the grafting reaction.

With more NaOH solution was added, α-1,4 glycosidic bond located in the starch molecule, tended to break in such a basic condition. At that time, the small sized molecule, glucose, was formed replacing the larger sized starch molecule. So far, glucose benefited the grafting reaction through a way of better diffusion and less steric hindrance, however, the amount of NaOH still needed to be controlled less than 3.9 g.

Table 3.5. Gel swelling ratio and G' versus various NaOH (aq) concentrations.

Specimen	NaOH concentration (g)	Swelling ratio (ml/ml)	G' (Pa)
PPG4-1	0	9	711
PPG4-2	0.98	8.5	1006.7
PPG4-3	1.95	8.3	1479
PPG4-4	2.93	8	1845
PPG4-5	3.9	10	896.9

In case of PPG4-5, excessive NaOH adjusted the aqueous solution to a highly basic condition in which AM was subjected to a sever hydrolysis, leading the system more hydrophilic but the gel less elastic. In general, a concentration of 2.93 g NaOH was recommended and exploited in the following investigations.

3.2.5. Optimization of MMT Concentration. Nanocomposite technology was acknowledged as a versatile technology for ameliorating polymer viscoelasticity, enhancing gel strength and improving thermal stability of polymeric materials. On the benchmark of precursor, polyacrylamide-grafting-starch (PAM-g-starch) gel, the nano sized sodium montmorillonite, was introduced and formulated with various concentrations.

Two mechanisms (Figure 3.16) dominated the interpretation about how nanoclay functioned in nanocomposite material; one is exfoliation and the other is intercalation [11].

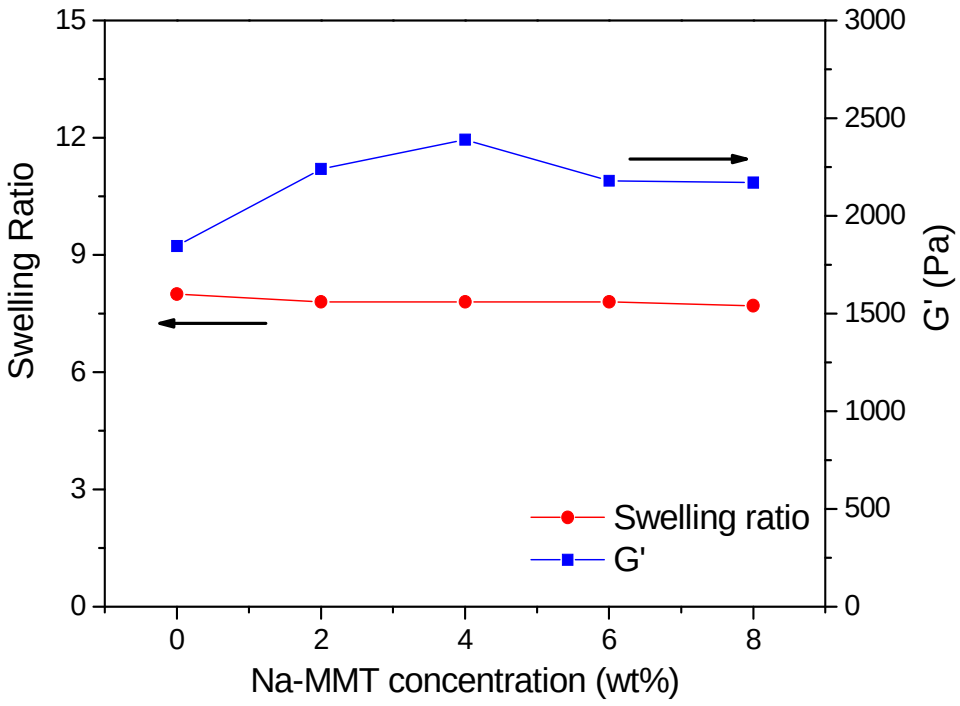

Figure 3.16. Gel swelling ratio and G' versus various MMT concentrations.

Based on our previous work [55], exfoliation was considered the predominating mechanism in this work. Figure 3.16 illustrated the impacts of various MMT concentration on gel swelling ratio and gel strength; the storage modulus (G') exhibited an increase once the amount of MMT was in the range of 2-4 gram. Herein, the MMT nanoparticles functioned as a physical crosslinker that associated with the negatively charged HPAM via electrostatic attraction. Owing to this association, a pseudo three-dimensional network formed as Figure 3.16 Mechanism I showing. What was more significant, the entanglement between polymer chains was strengthened.

In case that excessive MMT was added, such as PPG5-4 and PPG5-5, MMT performed not only a physical crosslinker but also a chain transfer agent that interfered chain propagation. Resulted by an increasing order of chain transfer reactions, the molecular weight, namely the chain length, decreased, leading to a decrement of chain entanglement and a less elastic polymeric network.

Taking account for both swelling ratio and gel strength, an appropriate MMT concentration was determined as 4 g.

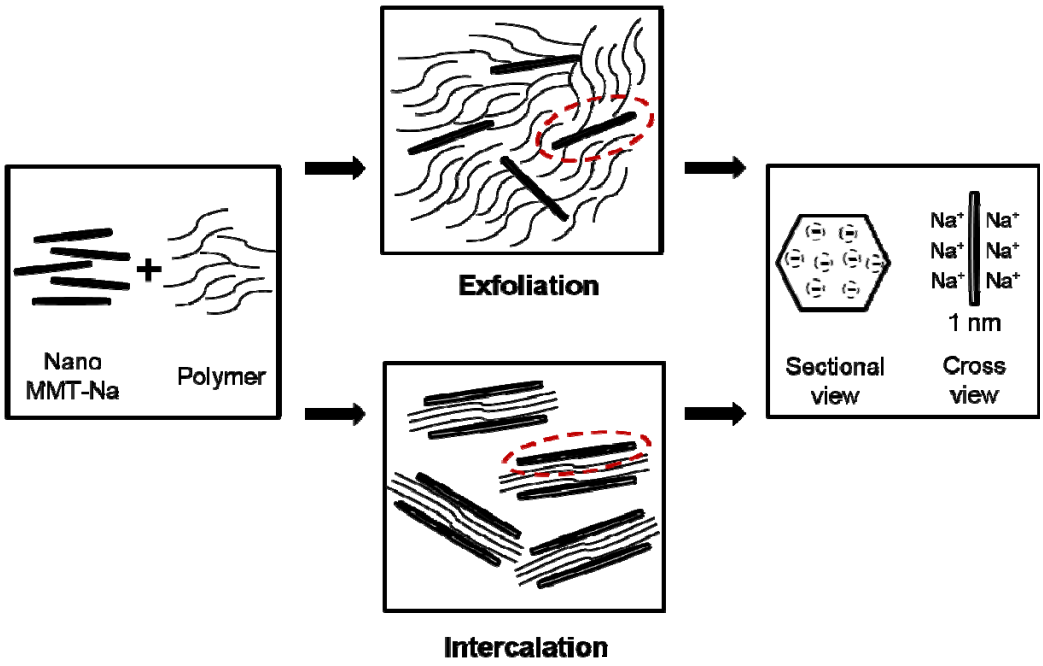

Figure 3.17. Two mechanisms exfoliation and intercalation of nanoclay compositing with PAM.

Table 3.6. Gel swelling ratio and G' versus various MMT concentrations.

Specimen	MMT concentration (g)	Swelling ratio (ml/ml)	G' (Pa)
PPG5-1	0	8	1845
PPG5-2	2	7.8	2240
PPG5-3	4	7.8	2390
PPG5-4	6	7.8	2180
PPG5-5	8	7.7	2170

3.2.6. Optimization of Other Additive Concentration. In this study, Na_2SO_3 solution (10 wt%) was introduced as a type of antifungals agent.

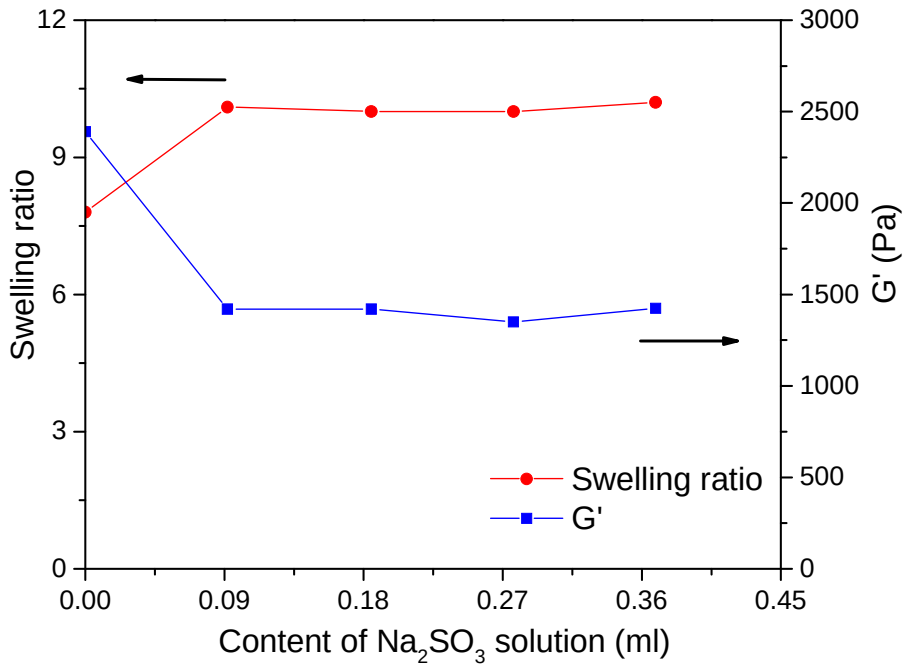

Figure 3.18. Gel swelling ratio and G' versus various additive concentrations.

In this study, Na_2SO_3 solution (10 wt%) was introduced as a type of antifungals agent. According to the result demonstrated by Figure 3.17, the gel strength (G') was impacted by the addition of this Na_2SO_3 solution. This phenomenon was caused by the sensitivity of nanoclay to sulfite group (SO_3^{2-}). Nanoclay, $(Na,Ca)_{0.33}(Al,Mg)_2(Si_4O_{10})(OH)_2 \cdot nH_2O$, as a type of layered silicate, contained various cations including Ca^{2+}, Mg^{2+}, Al^{3+} within its lattice. Once sulfite group and nanoclay encountered, these components was prone to forming association, thereby hindered attraction between HPAM and MMT.

Therefore, the optimum concentration of Na_2SO_3 solution was finalized at 0.19 g, and the recipe formulated PPG6-3 was considered the optimum formulation of starch-grafting-polyacrylamide nanocomposite gel.

Table 3.7. Gel swelling ratio and G' versus various additive concentrations.

Specimen	Na_2SO_3 concentration (g)	Swelling ratio (ml/ml)	G' (Pa)
PPG6-1	0	7.8	2390
PPG6-2	0.095	10.1	1420
PPG6-3	0.19	10	1420
PPG6-4	0.285	10	1350
PPG6-5	0.38	10.2	1425

3.2.7. Result of Core Flooding Test. In the first water flooding stage, owing to the existence of fracture, the injected brine easily and merely flooded along the fracture, featuring a low pressure gradient. Hardly sweeping the matrix, this deficient water flooding left a large portion of oil; only 3.691-13.031% OOIP was recovered, which was similar to what happened in the real development of heterogeneous reservoir [4].

During gel treatment, the pressure gradient revealed a continuous increase, denoting a successful migration and packing process of the injected gel particles [3]. Meanwhile, there appeared to be a leak-off yielded by the slight dehydration and free water from particle surface. Whereas, rather than an unfavorable effect, this leak-off did facilitate the recovery of remaining oil since more fracture adjacent area was swept.

In the second water flooding stage, the pressure gradient increased rapidly at the beginning. This rapid increase reflected an effective fracture blocking and plugging by which the gel pack intensively resistant the flow of chasing brine. A sudden drop followed, implying that the imposed pressure gradient reached the *breakthrough pressure* that SAC gel could withstand. After this leap, the pressure gradient partially resumed, which indicated wormholes or new flow paths have formed within the gel pack. By that time, the pressure gradient tended to stabilize, and thus a steady flow formed.

Beyond plugging performance, a pronounced increment of cumulative oil recovery was observed. This phenomenon supported that SAC particle gel did not only function in fracture remediation but also diverted chasing fluid. Injection brine was diverted into the matrix hence significantly improved the sweep efficiency, furthermore benefited the oil recovery.

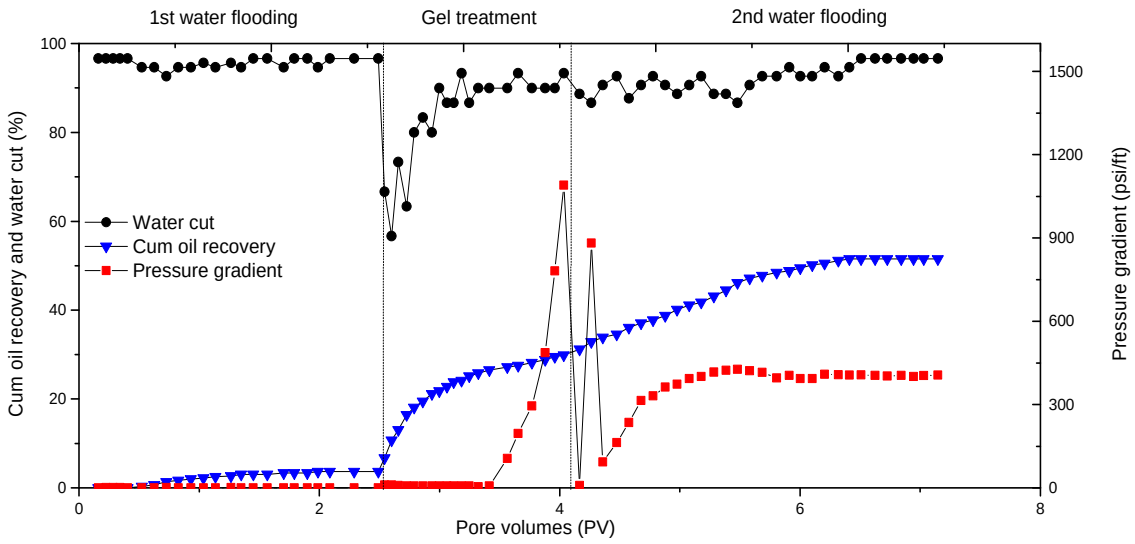

Figure 3.19. Core flooding result of core#1.

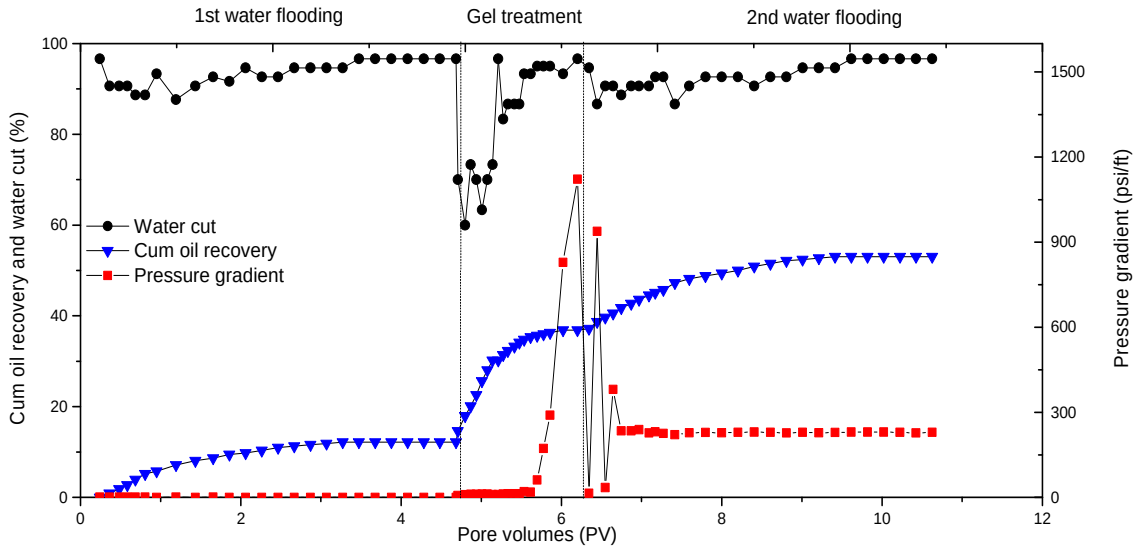

Figure 3.20. Core flooding result of core#2.

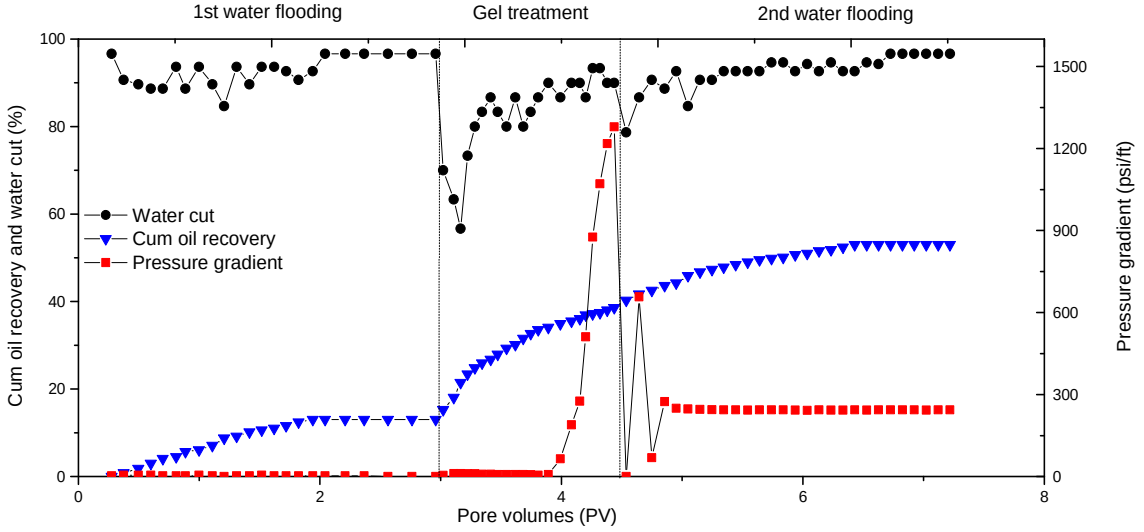

Figure 3.21. Core flooding result of core#3.

Residual resistance factor was calculated with the following equation in which P_a

$$F_{rr} = \frac{P_a}{P_b} \tag{2}$$

represented pressure difference before gel treatment, and P_b stood for pressure difference before gel treatment.

The incremental oil recovery was quantified via the following equation where E_S,

$$\Delta E = E_S - E_F \tag{3}$$

E_F represented cumulative oil recovery of second water flooding and first water flooding respectively.

Table 3.8. Results of core flooding tests.

Core code	Oil recovery (%)			Cumulative oil recovery (%)	Breakthrough pressure (psi/ft)	Frr
	1st water flooding	Gel treatment	2nd water flooding			
#1	3.69	26.17	21.64	51.51	881.66	1107.33
#2	12.19	24.69	16.15	53.04	937.80	630
#3	13.03	25.56	14.94	52.97	656.96	623.12

Given the Frr with such a large magnitude, SAC not only remedied the fracture effectively, but compared with the data reported previously and other commercial product [5][6], SAC gels were also indicated a robust plugging performance. Besides its superior elasticity, this robust plugging performance could be attributed to the formation of strong interaction between rock surface and SAC particles. As Figure 3.22 showing, hydrogen bonding formed due to the substantial existence of hydroxyl group (-OH) in starch chain and the silanol group (-SiO) on rock surface. In fact, this hydrogen bonding reinforced the retention for particles against *extrusion* from the open fracture, contributing in a robust plugging performance. It turned out that a core with a lower permeability, featured with higher Frr and increment oil recovery.

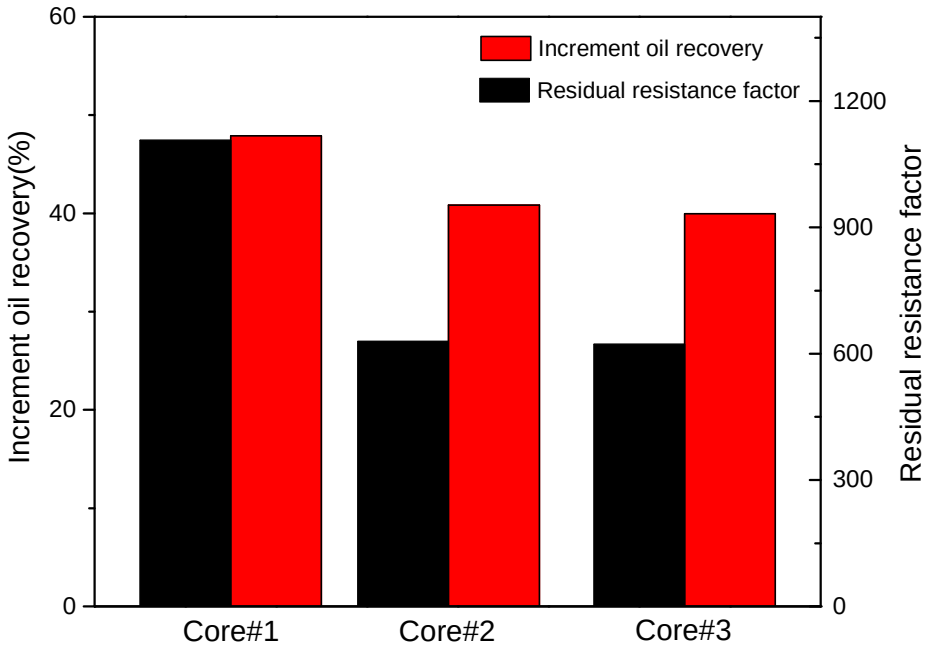

Figure 3.22. Comparison of incremental oil recovery and residual resistance factor among different cores.

Since Frr was determined by the ratio of the injection pressure after gel treatment (Pa) to the injection pressure before gel treatment (Pb), it would be prone to understanding Figure 3.21 based on fluid derivation and pressure variation.

As the fracture zone was blocked, the compacted gel pack had the chased brine flow redirected towards the core fragments. At that time, a less permeable core tended to impose larger flowing hindrance for the fluid. Consequently, higher pressure was required for diverting brine into such a low-permeability core which was more tight and impermeable. In contrast, it would be of more ease for injection brine to sweep a more permeable core.

For the other aspect, a higher $\boldsymbol{\Delta}E$ was obtained in the core with lower permeability. According to the oil recovery of first water flooding, core #1, #2, #3 characterized an oil recovery of 3.69, 12.20 and 13.03% respectively among which more remaining oil was left in the porous media of core 3 regardless its relatively low permeability. Provided this, the injection brine diverted by SAC gel treatment was more likely to recover more oil from core fragments with richer reserve.

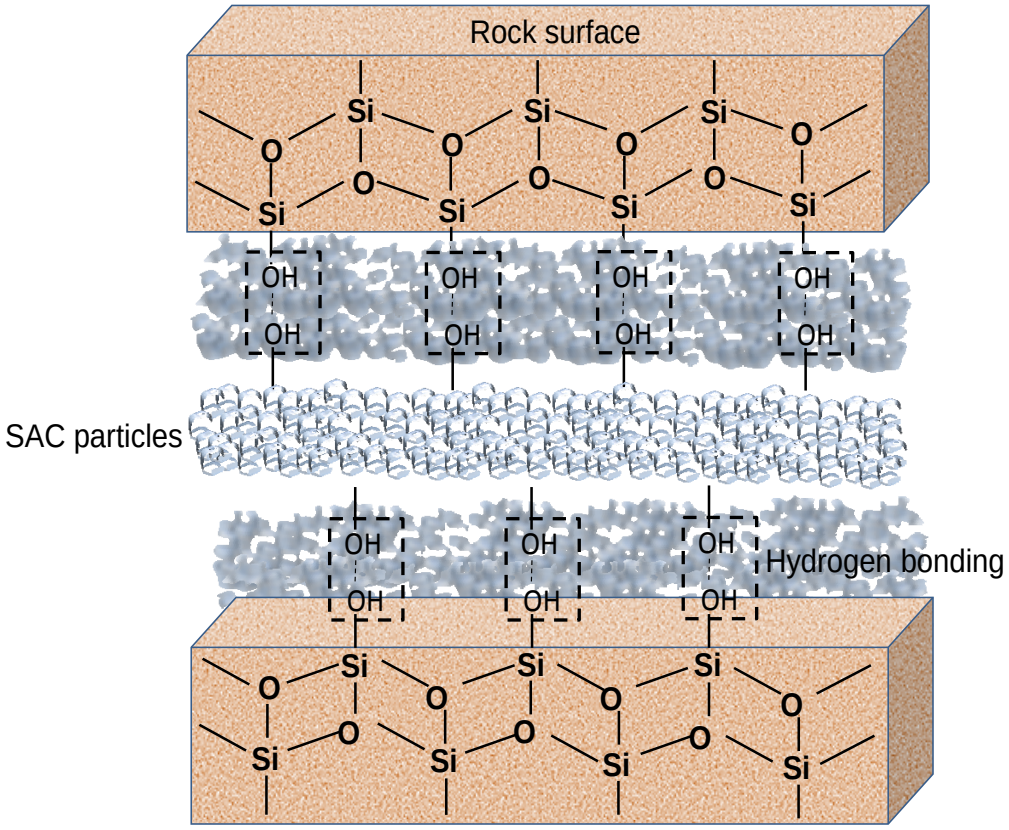

Figure 3.23. Schematic of hydrogen bonding formed between rock surface and SAC particles.

3.2.8. Characterization Results. The porous structures of both PAM and SAC could be observed (Figure 3.23 and 3.24), supporting the existence of three-dimensional network in these hydrogels. Comparing SEM image of PAM (Figure 3.23) with that of SAC (Figure 3.24 and 3.25), the distinguish was pronounced that microscale pore structure of PAM was relatively thin and rigid. However, microstructure of SAC appeared to be reinforced and more complex. As abovementioned, the special "encapsulation" configuration might account for this observation; since grafted onto the chain of PAM, starch attached, twined and encapsulated the polymeric matrix of PAM, making-up its original appearance.

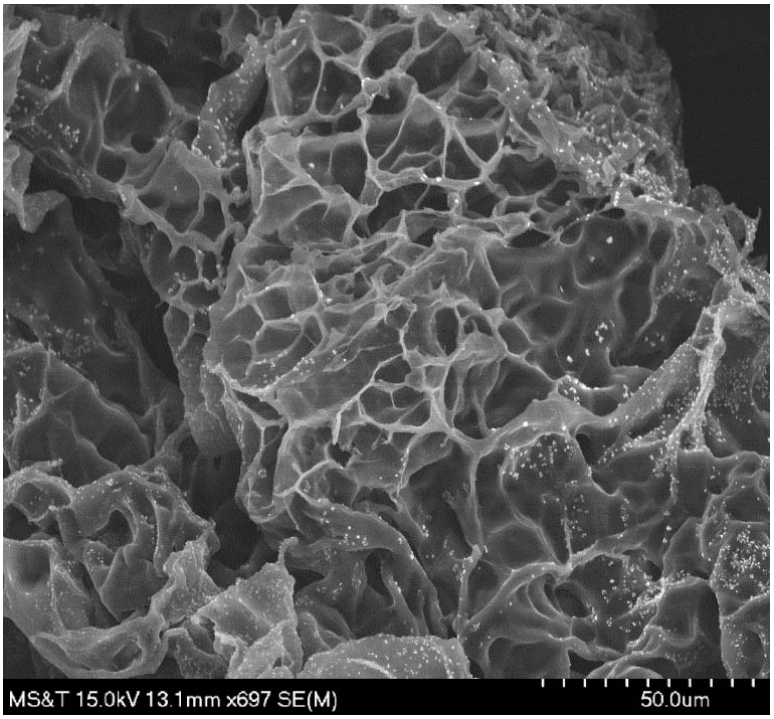

Figure 3.24. SEM image of PAM (I).

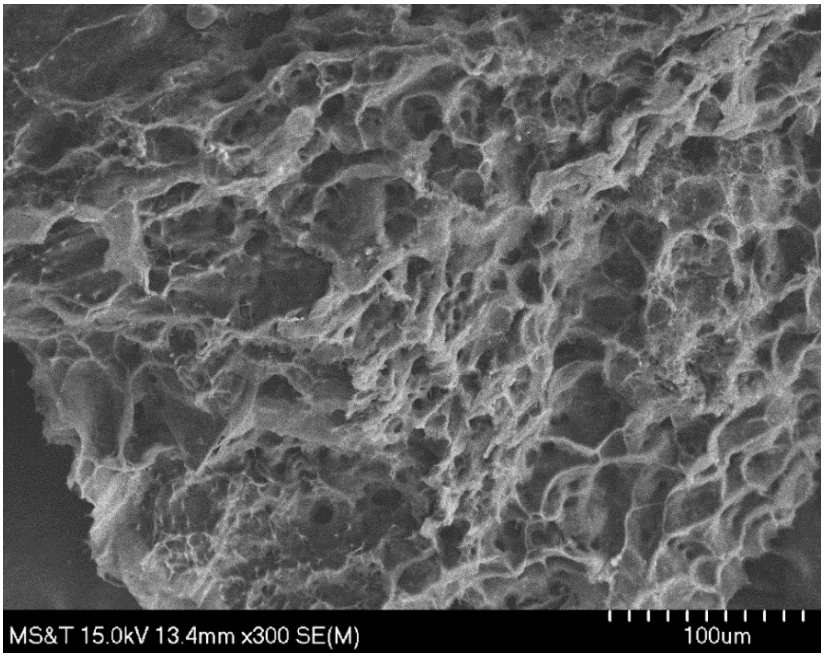

Figure 3.25. SEM image of SAC (II).

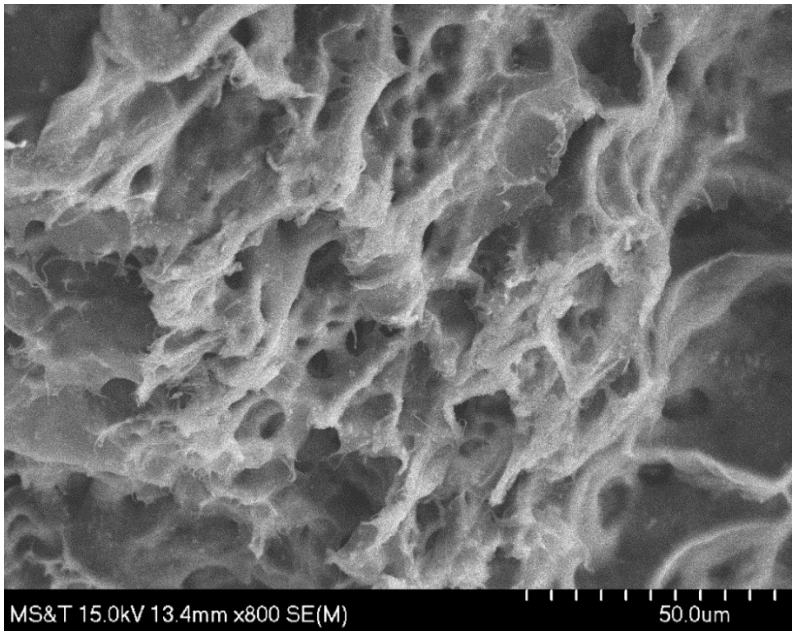

Figure 3.26. SEM image of SAC (II).

Infrared spectroscopy is a useful technique in characterizing structures of materials. The curve at the top of Figure 3.26 indicated the spectrum of pure PAM; the curve in the middle displayed the spectra of PAM-g-starch; and the curve at bottom showed the bands of SAC. A broad absorption band at 3352.52 cm^{-1} was caused by the NH stretching frequency of the NH_2 group. The peak at 2939 cm^{-1} and 2862 cm^{-1}, reflected the asymmetrical stretching vibration of -CH_2- group. The characteristic peaks at 1670 cm^{-1} , 1452 cm^{-1} and 1415 cm^{-1} were from the contribution of the C=O stretching (amide I), N-H bending, and C-N stretching respectively. For the spectra of AM-g-starch at peaks 2939, 1441, 1042 cm^{-1} were contributed by -CH2-, O-H, C-O, respectively. In the spectra of SAC, the absorption bands at 2932, 1668, 1608, 1310 cm^{-1} derived from -CH2- asymmetrical stretching vibration, C=O stretching(amide I band), N-H in plane bending in -$CONH_2$ group (amide II band) and C-N stretching, respectively. Bands at 1189 and 1122 cm^{-1} are corresponding to -NH_2-in-plane rocking vibration and the broad spectrum at 500 cm-1 is due to -NH_2- out-plane rocking vibration. Bands at 1441 and 1042 cm^{-1} showed up owing to O-H deformation and C-O stretching from starch's donation. Additionally, the absorption peak at 1430 cm-1 derived into two weak bands at

1451 and 1415 cm^{-1}, and the peak at 1096 cm^{-1} moved to low frequency 1122 cm^{-1}, which indicated that the production of free radical in –OH and partly copolymerize with AM monomer[36]. The results were suggesting that the preparation of SAC hydrogel, especially the incorporations of starch and MMT, did not have major structural transformations in comparison to the pure PAM hydrogel.

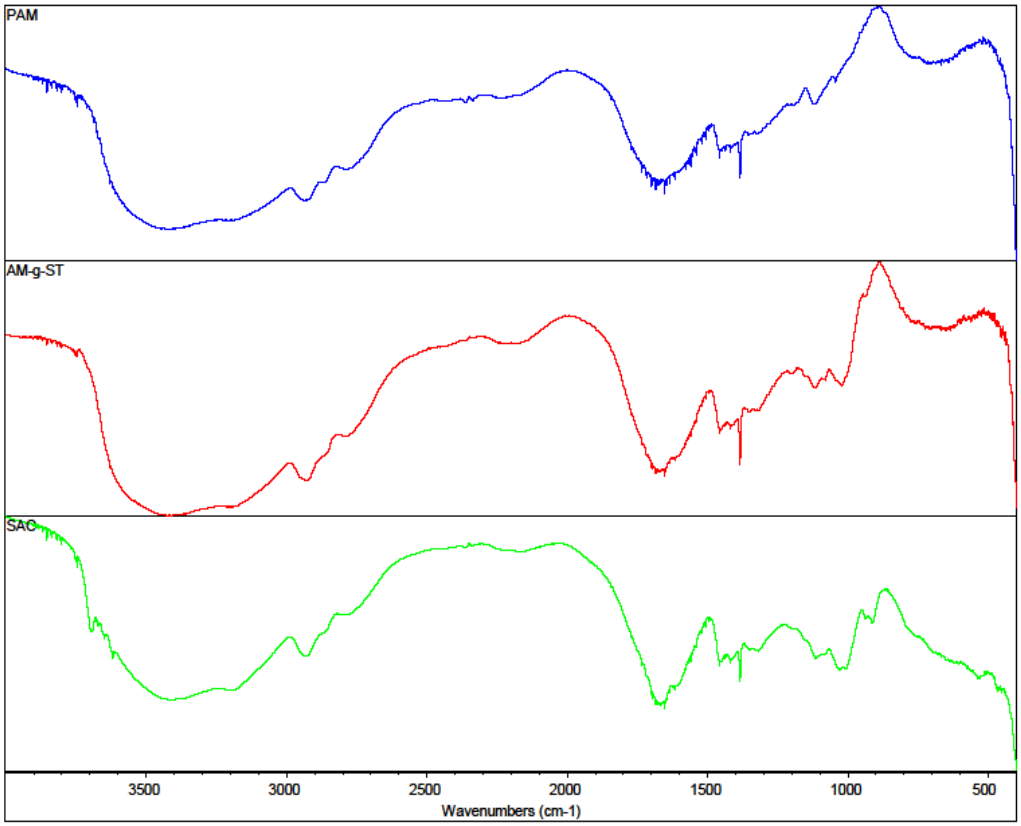

Figure 3.27. IR spectra of PAM (top), AM-g-starch (middle), and SAC (bottom).

4. RHEOLOGY STUDY AND CORE FLOODING TEST OF NOVEL PREFORMED PARTICLE GEL WITH INTERPENETRATING NETWORK

4.1. EXPERIMENTAL

Experimental study was initiated from the preparation of particle; followed by the evaluation of IPN; and finalized with a series of characterization.

4.1.1. Material and Preparation. The preparation of IPN was not detailed here but in another work [68]. Preparation of poly (vinyl alcohol)/polyacrylamide interpenetrating network hydrogel was carried out with commercially available monomers, initiators, and reagents. The monomer used in preparing the first network was acrylamide (AM, ≥98.0%, Alfa Aesar); Poly(vinyl alcohol) (PVA, molecular weight:78000 g/mol, 98.0% hydrolyzed, Sigma Aldrich) was used for formation of the second network; N, N′-methylene-bisacrylamide (MBA) (~99%, Sigma Aldrich) and glutaraldehyde (Grade II, 50 wt% in H2O, Sigma Aldrich) were employed as crosslinkers for AM and PVA respectively; Amonium persulfate (APS, ACS reagent, ≥98.0%, Sigma Aldrich) was used as initiator; Hydrogen chloride (HCl, Technical, Fisher Chemical) and sodium hydroxide (NaOH, Fisher Chemical) were used to adjust pH; Sodium chloride (NaCl, Fisher Chemical) was used to prepare brine water; Potassium bromide powder (KBr, ACS reagent, ≥99.0%, Fisher Chemical) was used for window material of Fourier Transform Infrared Spectroscopy.

4.1.2. Swelling Test. For preformed particle gels, swelling ratio is of great significance, which could affect on the injection amount, injection pressure and even applicable pore size. In term of swelling ratio, as volume is more highlighted in the real application of preformed particle gels, we assessed the swelling capacity of IPN gels via volumetric method expressed with following equation

Swelling behavior of IPN gels were investigated with different brines in ambient. 1 ml particles with a diameter of 0.6-0.85 mm were loaded into a tube, then merged with different brines. Herein, this constant volume, 1 ml, was considered as V_b. After a while, once the volume of swollen particles reached equilibrium, this volume was read as V_a and brought into the calculation.

4.1.3. Rheology Study. The rheology study was carried out using HAAKE MARS III (Germany) rheometer in ambient. The plate-plate geometry (PP35 Ti) was implemented, associating with a solvent trap to prevent vaporization. For a typical rheology study, specimen was usually tested in the form of bulk gel instead of particulate form. Thus, a piece of bulk IPN gel (without drying) first swelled in the brine followed by a crafting to the size of (12 mm*12 mm*3 mm); this disc-shape swelled bulk gel was performed with creep-recovery test. Two different phases comprised this creep–recovery test. Loading of a constant shear stress of 50 pa was kept for 600 seconds during which gel deformation was characterized; after an immediate remove of this stress, 300 more seconds without shearing were waited for a recovery of gel deformation. Eventually, a time dependent deformation result was achieved.

Figure 4.1. HAAKE MARSIII (Germany) rheometer.

4.1.4. Core Flooding Test. Procedures involving fracture preparation and flowing test were accomplished as following:

(1) The sandstone cores were oven dried at 120℃ for 24 hrs to remove the residual water. Then, a series of basic parameters including length (L), diameter (D), and dry weight (M) were measured in ambient.

(2) A specific core would be vacuumed for at least 4 hrs and then saturated with 1 wt% NaCl brine for 6 hrs. After brine saturation, a weight measurement was conducted to obtain the pore volume (PV) and porosity (φ).

(3) The core was mounted into the core holder and furtherly loaded with a constant overburden pressure of 500 psi. In order to specify the matrix permeability (K), 1 wt% NaCl brine was injected with four different flowrates (2.0 ml/min, 3.0 ml/min, 4.0 ml/min, 5.0 ml/min), while the real-time injection pressure was recorded. Until when steady-state flow was established, the matrix permeability (K) could be calculated via Darcy's law.

(4) The core was subsequently flooded by oil which possessed a viscosity of 14.3 cp in ambient. The injection flowrate was maintained at 0.8 ml/min thus the original oil saturation (OOIP) and irreducible water saturation (Swi) could be achieved.

(5) The oil-saturated core was taken out from the core holder. A longitudinal fracture was created along the core carefully and smoothly using a band saw. On the surface of one core segment, two identical pieces of incompressible steel (125 mm*50 mm*1.2 mm) were attached with adhesive agent. Once these two segments had been assembled, the entirety simulated the fracture aperture in which the steel performed as spacers to prop the fracture. One step further, we tied the segments up using Teflon® to ensure they had been assembled firmly.

(6) The core with artificial fracture was again mounted into the core holder followed by a brine injection with constant flowrate (2 ml/min). This process was considered as first water flooding (1st water flooding) in which brine was injected until the water cut reached as high as 98%. Meanwhile, the oil recovery was quantified through collecting the produced oil from outlet.

(7) Gel treatment was carried out after first water flooding. Swollen particle gels (0.44-0.74 mm) without free water had been placed in the accumulator and then injected into fracture aperture with a constant flowrate of 1 ml/min. Aiming at an effective fracture remediation, particle gels had been injected with an amount of 10 FV.

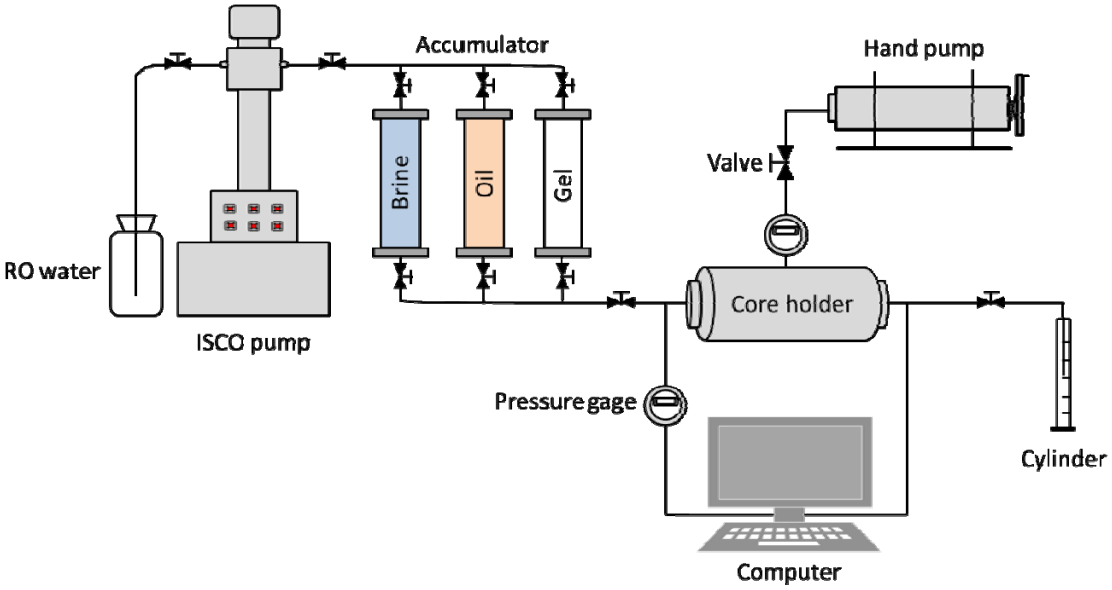

Figure 4.2. Experimental setting up of core flooding test.

Table 4.1. Parameters of sandstone cores for core flooding tests.

Core code	Length (mm)	Diameter (mm)	Matrix Permeability (md)	Porosity (%)	Pore volume (cm^3)	Fracture volume (cm^3)
#1	125.1	50.49	18.85	16.64	48.8	7.5
#2	125.0	50.51	156.0	16.54	48.9	7.5
#3	124.9	50.53	350.21	18.91	58.84	7.5

4.1.1. SEM Characterization. Morphology of IPN was characterized with Hitachi S-4700 Field Emission Scanning Electron Microscope (SEM). Swelled IPN particles (0.6-0.85 mm) were first frozen with liquid nitrogen which was followed by a 12 hour freezing-dry process. Then, the dried hydrogel networks were placed on a piece of conductive tape which was attached to the stainless steel stub, and sprayed with Au/Pd nano-particles for 3 min. SEM imaging was conducted using a field emitter source via a mixed detector at 15 kV accelerating voltage.

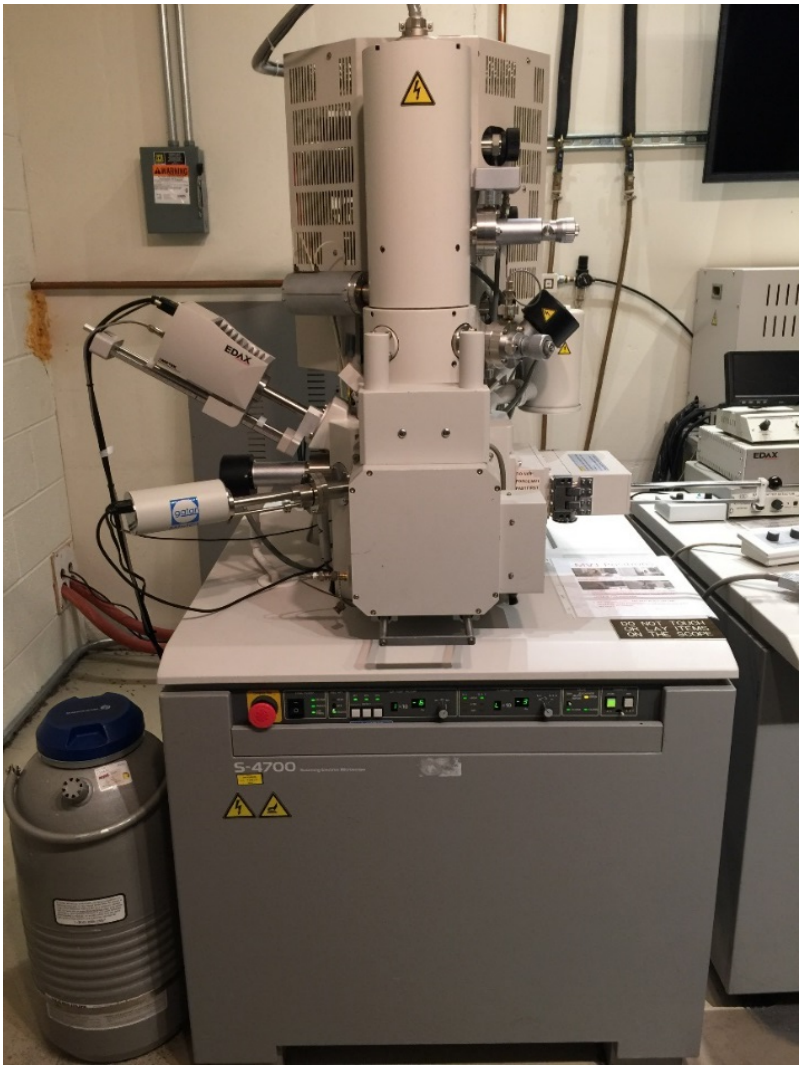

Figure 4.3. Hitachi S-4700 Field Emission Scanning Electron Microscope.

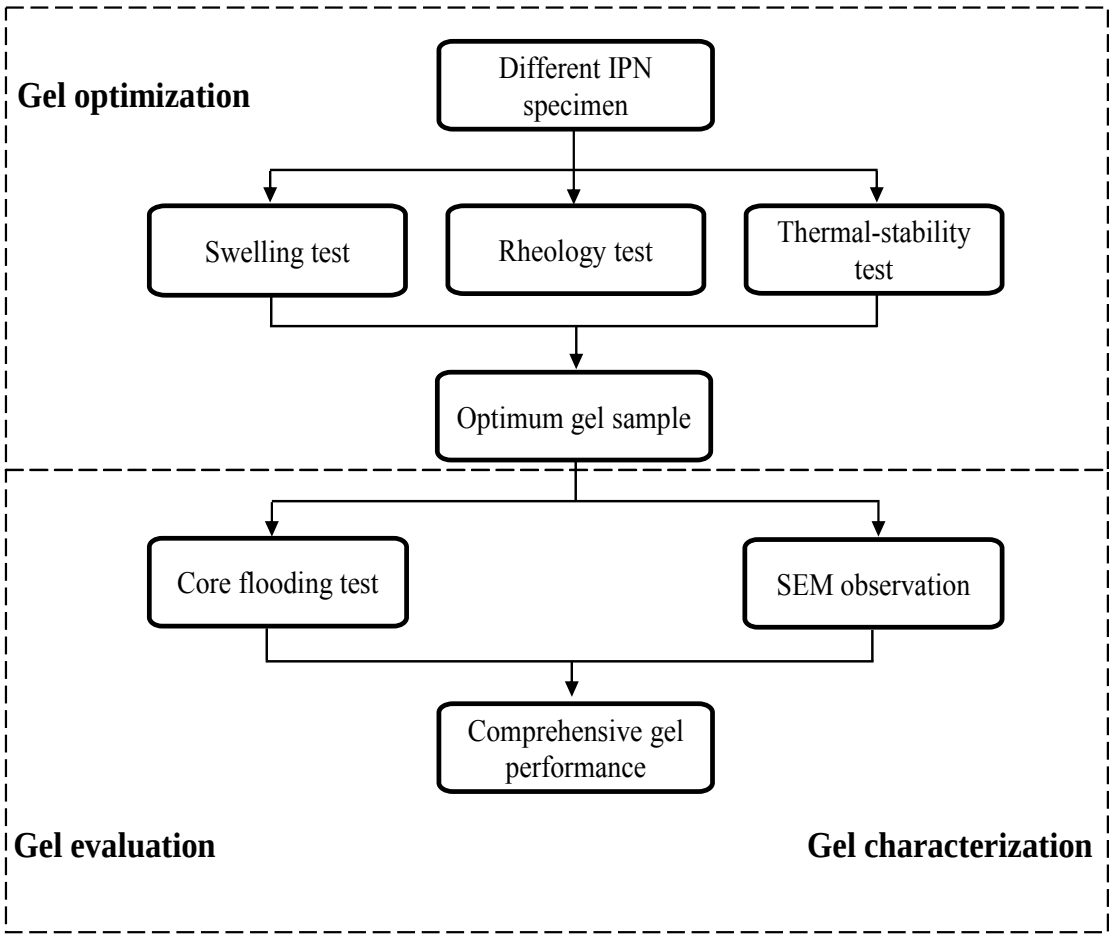

Figure 4.4. Schematic diagram of experimental steps.

4.2. RESULTS AND DISCUSSIONS

4.2.1. Result of Swelling Test. As the result showing in Figure 4.5, with an increase of PVA portion in IPN, the equilibrium swelling performance of the hydrogels deteriorated. The hydrophobicity of PVA portion might account for this deterioration. PVA chains contained the moiety of hydroxide group (-OH) which was relatively hydrophilic compared with the amide ($-CONH_2$) group in PAM. Thus, the hydrophobicity of entire system was enhanced due to the increasing of PVA. In addition, an introduction of PVA network condensed the original polymeric matrix established by PAM.

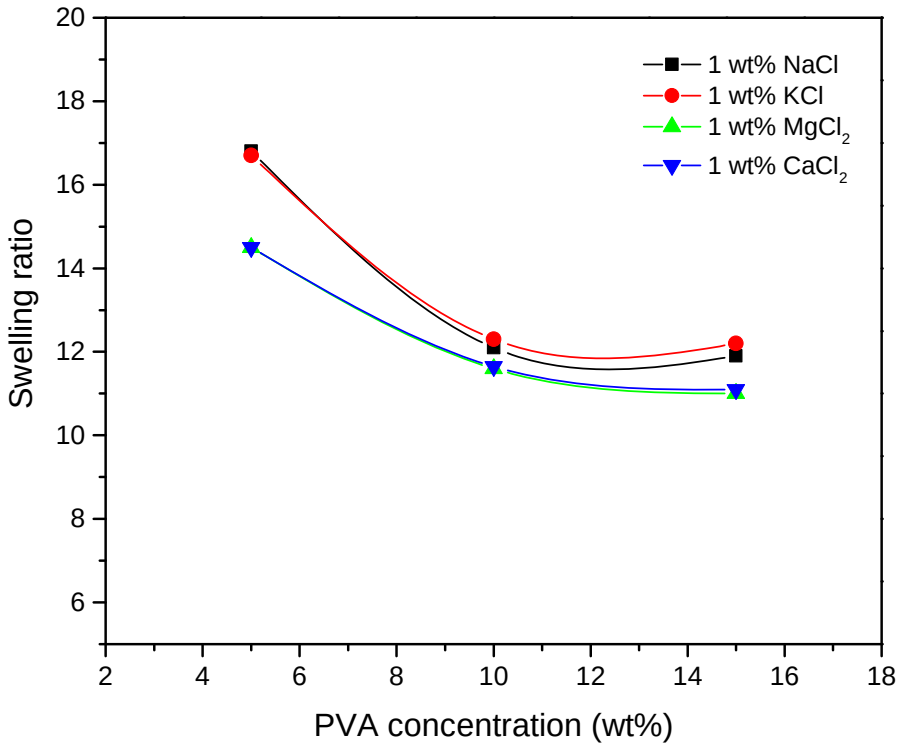

Figure 4.5. Swelling behavior of IPN and PAM in different brines.

4.2.2. Result of Rheology Study. Generally, rheological measurements involved two different methodologies, *Static Rheological Measurement* (SRM) and *Dynamic Rheological Measurement* (DRM). Different to SRM which was operated with a single-direction shear, DRM usually referred to a stepped shear or amplitude oscillation. In our previous study [2], amplitude oscillation as an important approach of DRM was employed to investigate the rheology properties of IPN gels. Beyond oscillation, another dynamic testing method, creep-recovery, has been implemented in this updated work. Creep-recovery featured with a stepped shear; it began with a constant stress imposed to specimen and accomplished with a stress releasement for material relaxation. A typical plot of creep-recovery test (Figure 4.6) was illustrated as followed. Within creep phase, the deformation initially revealed a repaid increase which is followed by a gradually decreasing slope of this strain curve [66]. Finally, this deformation (strain)-time curve might be lead to a constant tangent with a constant slope; the following recovery phase

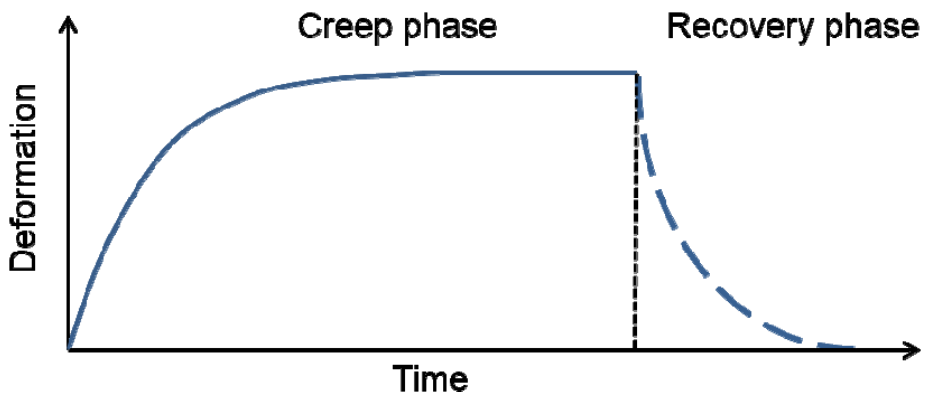

Figure 4.6. A typical plot of creep-recovery test with viscoelastic solid.

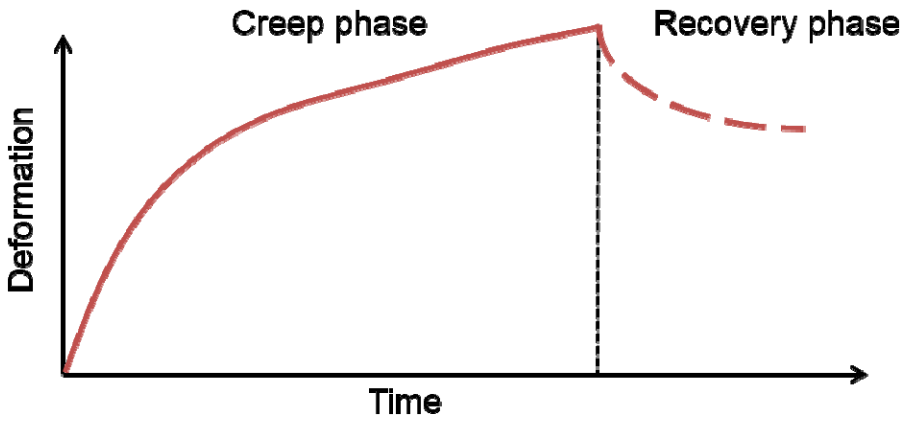

Figure 4.7. A typical plot of creep-recovery test with viscoelastic liquid.

also depended on time; once the applied stress was dismissed, only partial formation could be recovered due to a loss contributed to viscosity. Herein, the elasticity of testing specimen could be specified with the fraction of remained elastic portion.

$$Remained\ elastic\ portion = \frac{\gamma_{remained}}{\gamma_{\max imum}} \quad (4)$$

Thus, the elasticity of IPN gel was quantified with the following equation in which $\gamma_{remained}$ represented the recovered deformation (strain) and $\gamma_{maximum}$ related to the maximum deformation in creep phase.

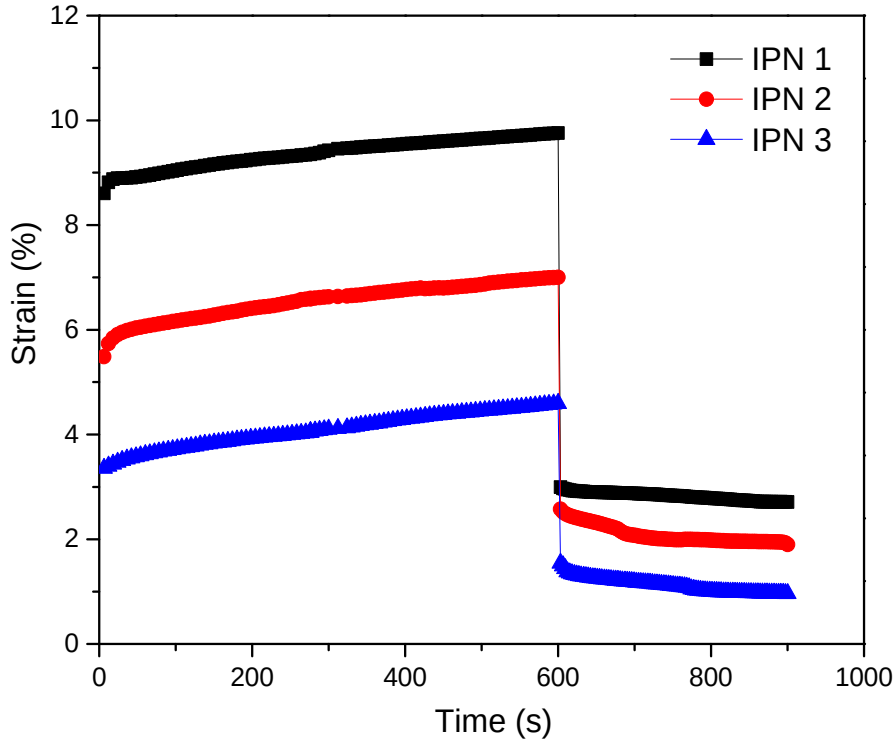

Figure 4.8. Creep test of IPN swelled in 1 wt% NaCl.

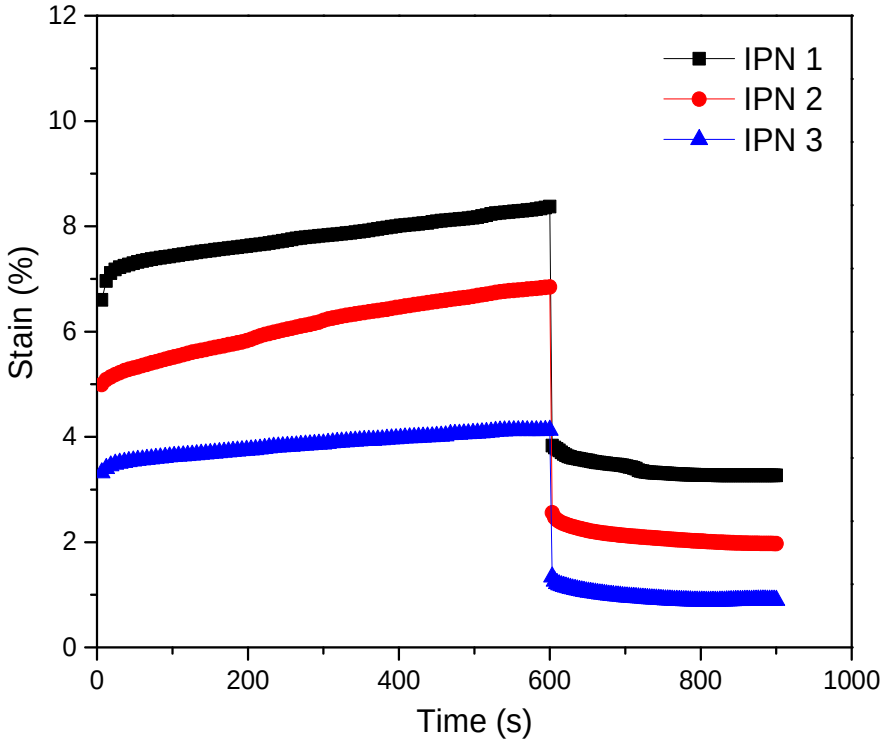

Figure 4.9. Creep test of IPN swelled in 1 wt% KCl.

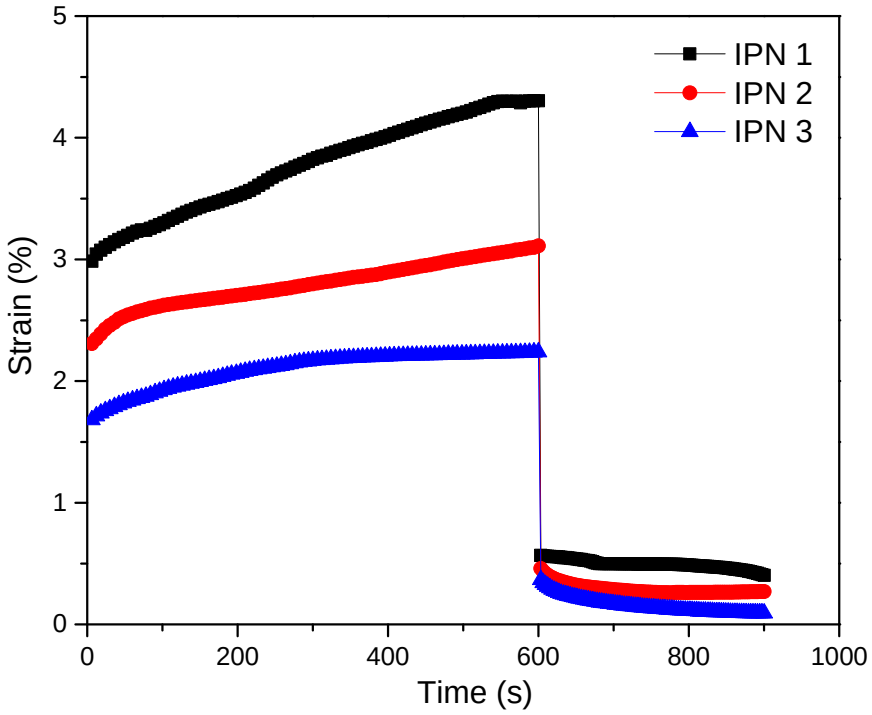

Figure 4.10. Creep test of IPN swelled in 1 wt% $CaCl_2$.

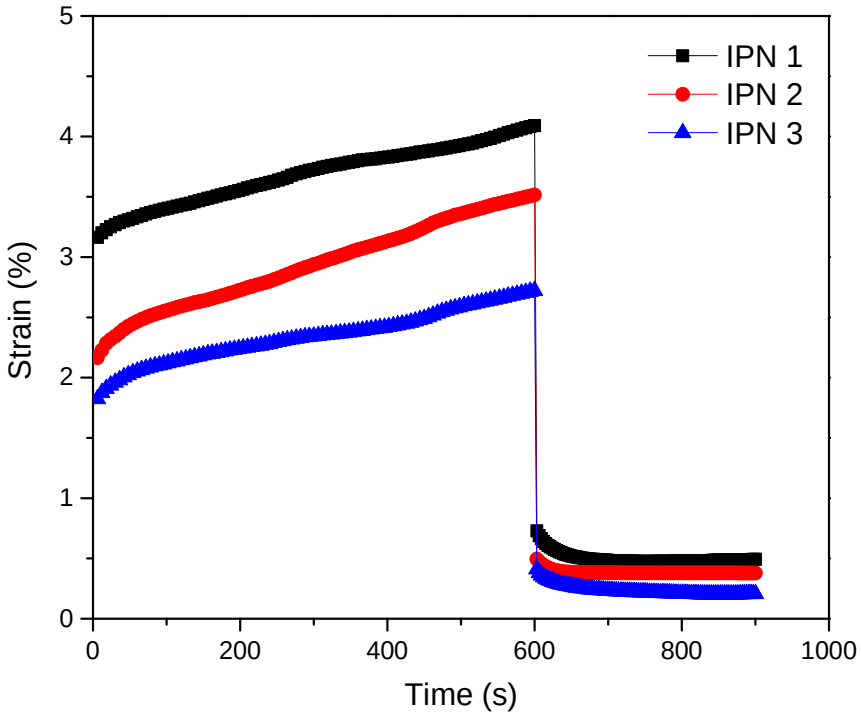

Figure 4.11. Creep test of IPN swelled in 1 wt% $MgCl_2$.

Table 4.2. Results of creep test.

	Specimen	Brine			
		1 wt% NaCl	1 wt% KCl	1 wt% $CaCl_2$	1 wt% $MgCl_2$
Ultimate deformation (%)	IPN 1	9.76	8.37	4.30	4.10
	IPN 2	7.0	6.85	3.11	3.52
	IPN 3	4.59	4.13	2.24	2.72
Remained elastic portion (%)	IPN 1	72.21	61.0	90.65	87.95
	IPN 2	72.87	71.21	91.31	89.21
	IPN 3	79.02	78.26	95.89	92.42

It was observed that if there was higher PVA concentration in IPN system, that hydrogel would become less deformable.

Likewise, the result of creep-recovery also indicated that with an increase of PVA concentration, the IPN gels characterized a higher $\gamma_{remained}$, implying that IPN gels became more elastic.

At the meantime, IPN gels swelled in divalent salt brine presented more elastic than those swelled in monovalent salt brine.

4.2.3. Result of Core Flooding Test. In the first water flooding stage, owing to the existence of fracture, the injected brine easily and merely flooded along the fracture, featuring a low pressure gradient. Hardly sweeping the matrix, this deficient water flooding left a large portion of oil; only 4.123-14.126 % was recovered, which was similar to what happened in the real development of heterogeneous reservoir [69].

During gel treatment, the pressure gradient revealed a continuous increase, denoting a successful migration and packing process of the injected gel particles[68]. Meanwhile, there appeared to be a leak-off yielded by the slight dehydration and free water from particle surface. Whereas, rather than an unfavorable effect, this leak-off did facilitate the recovery of remaining oil since more fracture adjacent area was swept. In the second water flooding stage, the pressure gradient increased rapidly at the beginning. This rapid increase reflected an effective fracture blocking and plugging by which the gel pack intensively resistant the flow of chasing brine. A sudden drop followed, implying that the imposed pressure gradient reached the *breakthrough pressure* that IPN gel could withstand. After this leap, the pressure gradient partially resumed, which indicated along the fracture, wormholes or new flow paths have formed within the gel pack. By that time, the pressure gradient tended to stabilize, and thus a steady flow formed.

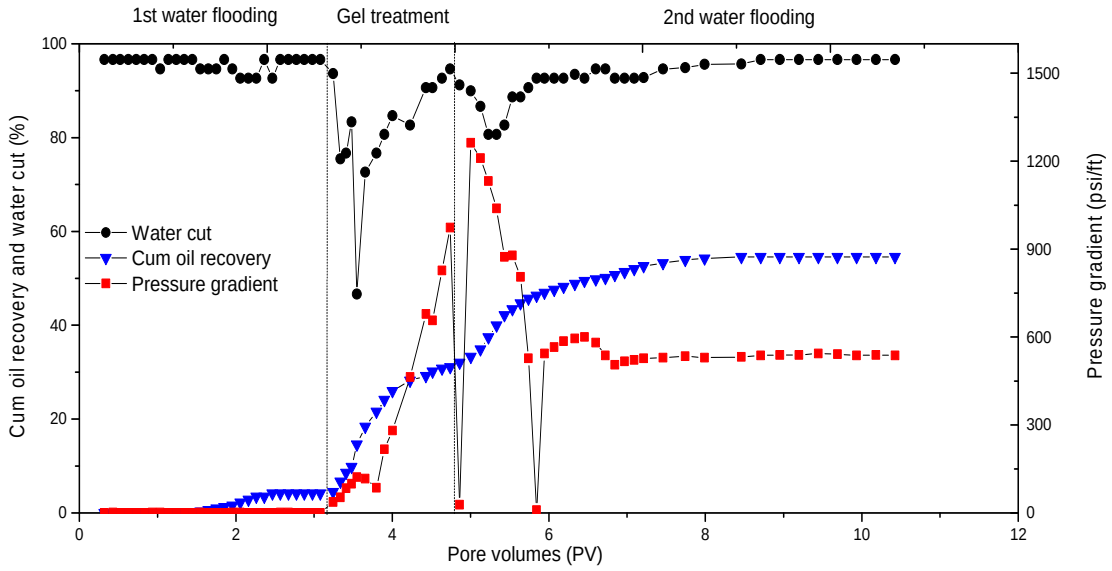

Figure 4.12. Core flooding test with core#1.

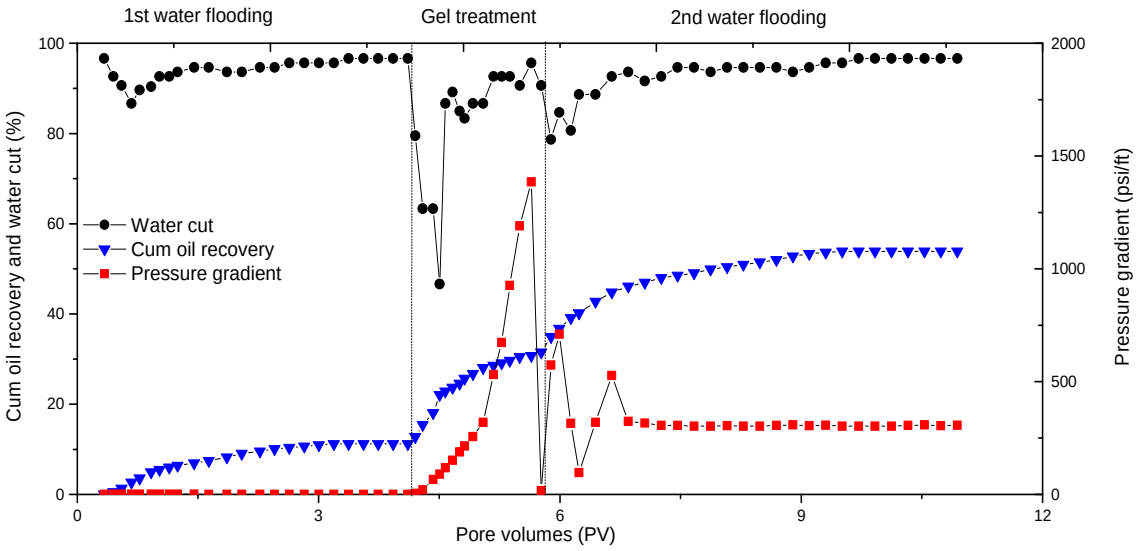

Figure 4.13. Core flooding test with core#2.

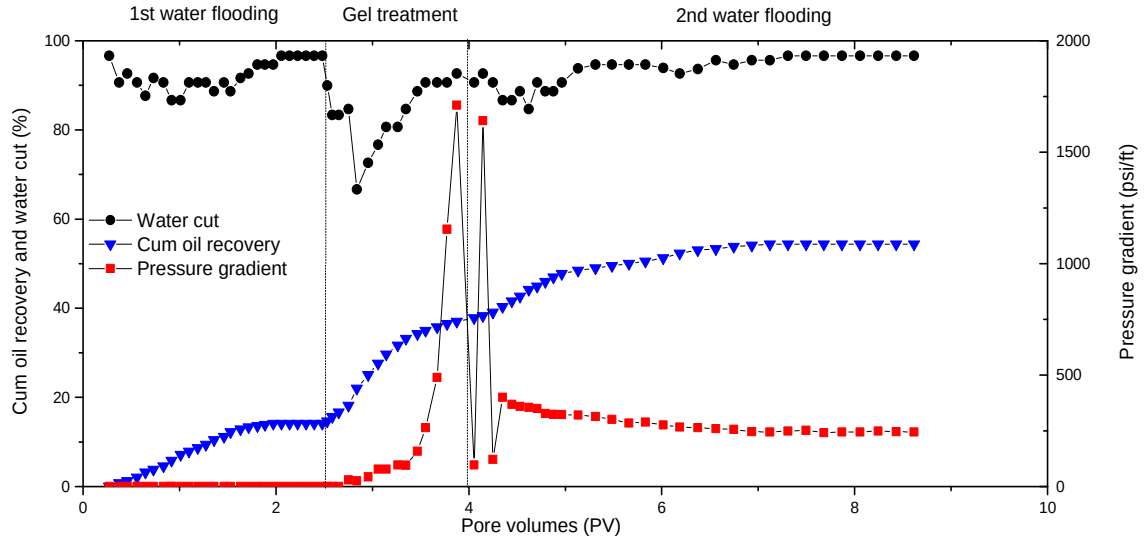

Figure 4.14. Core flooding test with core#3.

Beyond plugging performance, a pronounced increment of cumulative oil recovery was observed. This phenomenon supported that IPN did not only function in fracture remediation but also diverted chasing fluid. Injection brine was diverted into the

matrix hence significantly improved the sweep efficiency, furthermore benefited the oil recovery.

Table 4.3. Results of core flooding tests.

Core code	Oil recovery (%)			Cumulative oil recovery (%)	Breakthrough pressure (psi/ft)	F_{rr}
	1st water flooding	Gel treatment	2nd water flooding			
#1	4.12	26.96	23.47	54.55	1262	2200.04
#2	11.17	19.55	23.15	53.87	709.76	1046.67
#3	14.13	22.91	17.31	54.34	1641.81	910.91

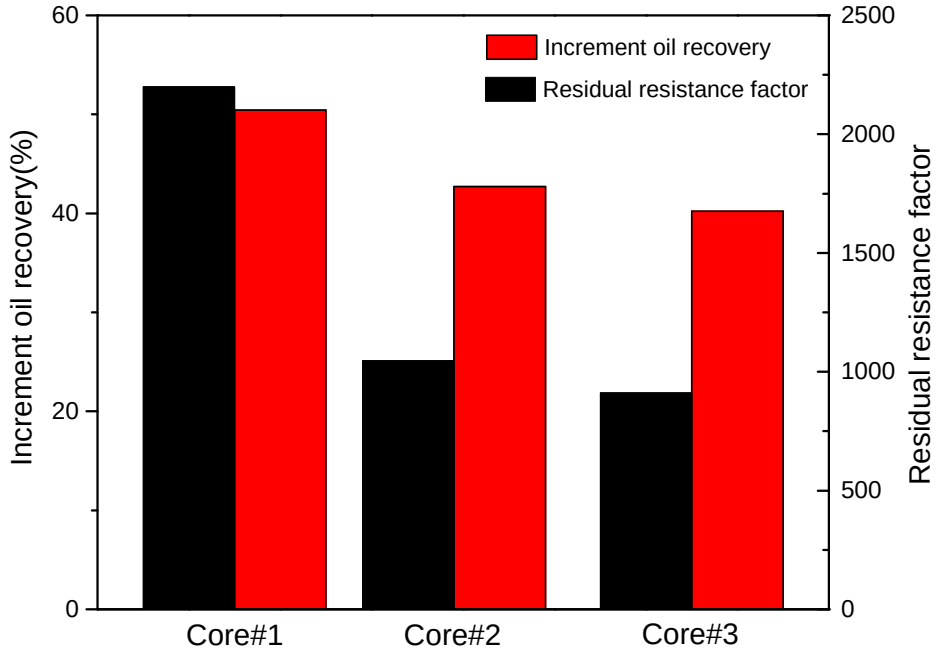

Figure 4.15. Increment oil recovery and Residual resistance factor of each fractured core.

Given the F_{rr} with such a large magnitude, IPN not only remedied the fracture effectively, but compared with the data reported previously [70][71], IPN gels were also indicated a superior plugging performance.

It turned out that a core with a lower permeability, featured with higher F_{rr} and increment oil recovery. Since F_{rr} was determined by the ratio of the injection pressure after gel treatment (Pa) to the injection pressure before gel treatment (P_b), it would be prone to understanding Figure 4.14 based on fluid derivation and pressure variation.

As the fracture zone was blocked, the compacted gel pack had the chased brine flow redirected towards the core fragments. At that time, a less permeable core tended to impose larger flowing hindrance for the fluid. Consequently, higher pressure was required for diverting brine into such a low-permeability core which was more tight and impermeable. In contrast, it would be of more ease for injection brine to sweep a more permeable core.

For the other aspect, a higher $\boldsymbol{\Delta E}$ was obtained in the core with lower permeability. According to the oil recovery of first water flooding, core #1, #2, #3 characterized an oil recovery of 4.123, 11.17, and 14.126% respectively among which more remaining oil was left in the porous media of core 3 regardless its relatively low permeability. Provided this, the injection brine diverted by IPN gel treatment was more likely to recover more oil from core fragments with richer reserve.

4.2.4. Result of SEM Characterization. Porosity is tightly correlated with mechanical performance of a matrix as it affects the applications such as encapsulation of other materials. The synthesized PAM hydrogel and PAM/PVA IPN had a highly porous structure (Figure 4.17), which would favor effective absorption of water or other materials. The SEM images clearly demonstrated the morphological difference when PVA added into system. From Figure 4.17, IPN gel exhibited obvious secondary network. Mishra et al reported their work on PAM/PVA semi IPNs, in which linear PVA polymer was embedded in polyacrylamide network without further crosslinking. No obvious porous structure were observed in their SEM micrographs and it was claimed that with increasing content of AM in semi-IPN, hydrogels' surface acquired increasing heterogeneity.

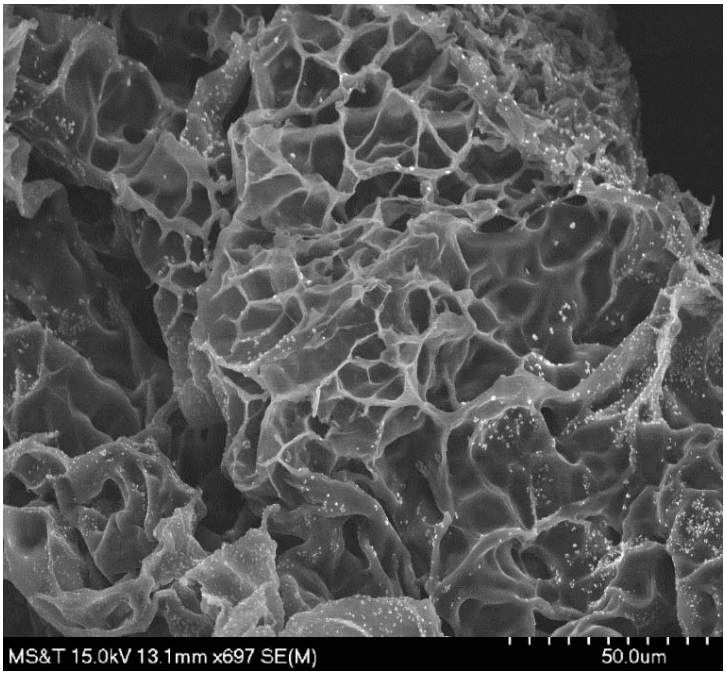

Figure 4.16. SEM micrograph of PAM.

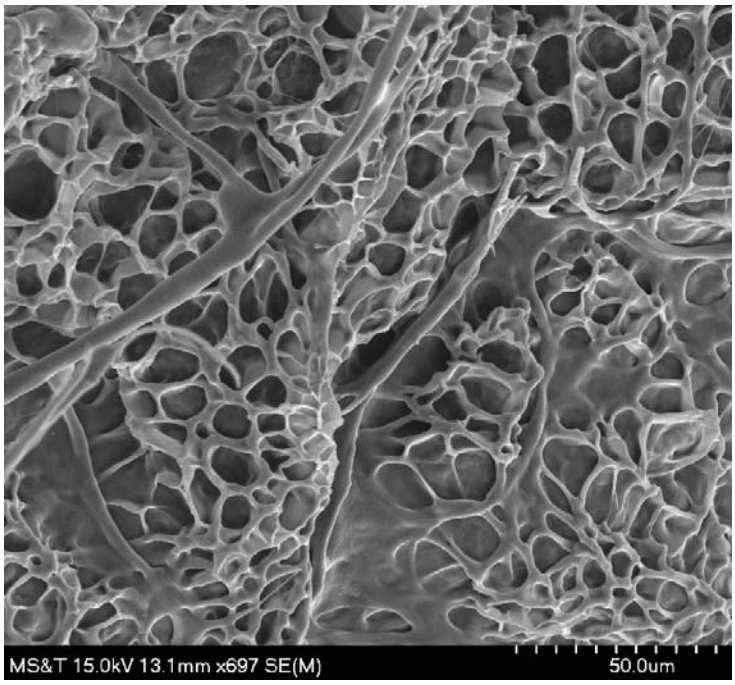

Figure 4.17. SEM micrograph of IPN.

5. CONCLUSION

Novel material, Starch-grafting-Poly(acrylamide)/ Nano-Composite (SAC) hydrogel, was successfully synthesized using free redial polymerization. The optimum specimen of novel preformed particle gel, SAC gels, were achieved through investigating and comparing the impacts of internal factors. Effects of external factors were thoroughly studied based on comprehensive evaluations. It turned out that SAC gel was much stronger than conventional PPG in which the G' was promoted from 360.8 pa to 1414 pa. Both rheology properties and thermal stability were intensively improved due to the addition nano-clay.

The possibility of SAC particle gels as plugging agent for conformance control has been studied by plugging test with fractured sandstone cores. It was indicated that the treatment using SAC particle gels could effectively remedy the fracture taking advantage of strong retention, meanwhile enhance the recovery of remaining oil. Moreover, SAC treatment characterized a more favorable plugging performance in lower permeability sandstone core which supported the application of SAC for low permeability fractured reservoir.

PAM/PVA IPN gels which contained a high strength network of polyacrylamide and poly vinyl alcohol were successfully prepared. A series of compatible PVA/PAM IPN hydrogels were prepared by in situ free radical solution polymerization/crosslinking of AM and methylene-bisacrylamide, meanwhile crosslinking PVA in with glutaraldehyde. As a result of secondary PVA network in PAM hydrogel, the rheology properties had been enhanced greatly. It is shown that the IPN hydrogel matrix fabricated may easily be tuned in terms important parameters such as mechanical strength, swelling and porosity as per need by varying composition, thus fulfilling specific application requirements. The possibility of PAM/PVA IPN hydrogels as plugging agent for EOR has been studied by plugging test with fractured sandstone core.

BIBLIOGRAPHY

1. Okumura, Y., & Ito, K. (2001). The polyrotaxane gel: a topological gel by figure-of-eight crosslinks. *Advanced Materials*, 13(7), 485–487.

2. GelKarino, T., Okumura, Y., Zhao, C., Kataoka, T., Ito, K., & Shibayama, M. (2005). SANS studies on deformation Mechanism of slide-ring gel. *Macromolecules*, 38(14), 6161–6167.

3. Harada, A., Hashidzume, A., Yamaguchi, H., & Takashima, Y. (2009). Polymeric rotaxanes. *Chemical Reviews*, 109, 5974–6023.

4. Liu, Y., Fan, Z., Zhang, H. Y., & Diao, C. H. (2003). Binding ability and self-assembly behavior of linear polymeric supramolecules formed by modified β-Cyclodextrin. *Organic Letters*, 5(6), 251–254.

5. Kjøniksen, A. L., Beheshti, N., Kotlar, H. K., Zhu, K., & Nyström, B. (2008). Modified polysaccharides for use in enhanced oil recovery applications. *European Polymer Journal*, 44(4), 959–967.

6. Liu, X., Jiang, W., Gou, S., Ye, Z., Feng, M., Lai, N., & Liang, L. (2013). Synthesis and evaluation of novel water-soluble copolymers based on acrylamide and modular β-cyclodextrin. *Carbohydrate polymers*, 96(1), 47-56.

7. Liu, X., Jiang, W., Gou, S., Ye, Z., & Luo, C. (2013). Synthesis and clay stabilization of a water-soluble copolymer based on acrylamide, modular β-cyclodextrin, and AMPS. *Journal of Applied Polymer Science*, 128(5), 3398–3404.

8. Qin, Y., Zou, C., Yan, X., Zhou, L., & Luo, P. (2015). High performance acid composition based on cationic β-cyclodextrin inclusion complexes for enhancing oil recovery. *Chemical Engineering Research and Design*, 94, 301-306.

9. Zou, C., Qin, Y., Yan, X., Zhou, L., & Luo, P. (2014). Study on Acidizing Effect of Cationic β-Cyclodextrin Inclusion Complex with Sandstone for Enhancing Oil Recovery. Industrial & Engineering Chemistry Research, 53(33), 12901-12910.

10. Zou, C., Zhao, P., Hu, X., Yan, X., Zhang, Y., Wang, X., & Luo, P. (2013). β-Cyclodextrin-functionalized hydrophobically associating acrylamide copolymer for enhanced oil recovery. *Energy & Fuels*, 27(5), 2827-2834.

11. Wei, B., Romero-Zerón, L., & Rodrigue, D. (2014). Formulation of a self-assembling polymeric network system for enhanced oil recovery applications. *Advances in Polymer Technology*, 33(3).

12. Wei, B., Romero-Zeron, L., & Rodrigue, D. (2014). Evaluation of two new self-assembly polymeric systems for enhanced heavy oil recovery. *Industrial & Engineering Chemistry Research*, 53(43), 16600-16611.

13. Wei, B., Romero-Zerón, L., & Rodrigue, D. (2014). Novel self-assembling polymeric system based on a hydrophobic modified copolymer: formulation, rheological characterization, and performance in enhanced heavy oil recovery. *Polymers for Advanced Technologies*, 25(7), 732-741.

14. Wei, B., Romero-Zerón, L., & Rodrigue, D. (2015). Improved viscoelasticity of xanthan gum through self-association with surfactant: β-cyclodextrin inclusion complexes for applications in enhanced oil recovery. *Polymer Engineering & Science*, 55(3), 523-532.

15. Wei, B. (2015). β-Cyclodextrin associated polymeric systems: Rheology, flow behavior in porous media and enhanced heavy oil recovery performance. *Carbohydrate polymers*, 134, 398-405.

16. Gong, J. P., Katsuyama, Y., Kurokawa, T., & Osada, Y. (2003). Double-network hydrogels with extremely high mechanical strength. *Advanced Materials*, 15(14), 1155-1158.

17. Shuler, P. J. (2011). *Novel Self-Thickening Chemicals for Improved Conformance Control (No. SC0004194)*. ChemEOR, Inc.

18. Seright, R. S., & Liang, J. (1995, January). A comparison of different types of blocking agents. In *SPE European Formation Damage Conference*. Society of Petroleum Engineers.

19. Haraguchi, K., & Takehisa, T. (2002). Nanocomposite hydrogels: a unique organic-inorganic network structure with extraordinary mechanical, optical, and swelling/de-swelling properties. *Advanced Materials*, 14(16), 1120.

20. Haraguchi, K., & Juan-Jun, L. (2004). Mechanical Properties of Nano-composite Hydrogels Consisting of Organic/Inorganic Networks and the Effects of Clay Modification thereto. *JOURNAL OF NETWORK POLYMER JAPAN*, 25(1), 2-12.

21. Haraguchi, K. (2011). Synthesis and properties of soft nanocomposite materials with novel organic/inorganic network structures. *Polymer journal*, 43(3), 223-241.

22. Haraguchi, K., Li, H. J., Matsuda, K., Takehisa, T., & Elliott, E. (2005). Mechanism of forming organic/inorganic network structures during in-situ free-radical polymerization in PNIPA-clay nanocomposite hydrogels. *Macromolecules*, 38(8), 3482-3490.

23. Haraguchi, K. (2007). Nanocomposite hydrogels. *Current Opinion in Solid State and Materials Science*, 11(3), 47-54.

24. Sydansk, R. D., & Moore, P. E. (1992). Gel conformance treatments increase oil production in Wyoming. *Oil and Gas Journal;(United States)*, 90(3).

25. Seright, R. S. (2004). Conformance improvement using gels. *Annual Technical Progress Report (US DOE Report DOE/BC/15316-6), US DOE Contract DE-FC26-01BC15316 (Sept. 2004), 72.*

26. Al-Anazi, H. A., & Sharma, M. M. (2002, January). Use of a pH sensitive polymer for conformance control. In *International Symposium and Exhibition on Formation Damage Control*. Society of Petroleum Engineers.

27. Huh, C., Choi, S. K., & Sharma, M. M. (2005, January). A Rheological Model for pH-Sensitive Ionic Polymer Solutions for Optimal Mobility Control Applications. In *SPE annual technical conference and exhibition*. Society of Petroleum Engineers.

28. Chauveteau, G., Omari, A., Tabary, R., Renard, M., Veerapen, J., & Rose, J. (2001, January). New size-controlled microgels for oil production. In *SPE international symposium on oilfield chemistry*. Society of Petroleum Engineers.

29. Rousseau, D., Chauveteau, G., Renard, M., Tabary, R., Zaitoun, A., Mallo, P., & Omari, A. (2005, January). Rheology and transport in porous media of new water shutoff/conformance control microgels. In SPE *international symposium on oilfield chemistry*. Society of Petroleum Engineers.

30. Zaitoun, A., Tabary, R., Rousseau, D., Pichery, T. R., Nouyoux, S., Mallo, P., & Braun, O. (2007, January). Using microgels to shut off water in a gas storage well. In *International Symposium on Oilfield Chemistry*. Society of Petroleum Engineers.

31. Pritchett, J., Frampton, H., Brinkman, J., Cheung, S., Morgan, J., Chang, K. T., & Goodgame, J. (2003, January). Field application of a new in-depth waterflood conformance improvement tool. In SPE *international improved oil recovery conference in Asia Pacific*. Society of Petroleum Engineers.

32. Frampton, H., Morgan, J. C., Cheung, S. K., Munson, L., Chang, K. T., & Williams, D. (2004, January). Development of a novel waterflood conformance control system. In *Spe/doe Symposium on Improved Oil Recovery*. Society of Petroleum Engineers.

33. Coste, J. P., Liu, Y., Bai, B., Li, Y., Shen, P., Wang, Z., & Zhu, G. (2000, January). In-Depth Fluid Diversion by Pre-Gelled Particles. Laboratory Study and Pilot Testing. In *SPE/DOE improved oil recovery symposium*. Society of Petroleum Engineers.

34. Bai, B., Li, L., Liu, Y., Liu, L., Wang, Z., & You, C. (2007). Conformance Control by Preformed Particle Gel: Factors Affecting It Properties and Applications, *SPE Reservoir Evaluation & Engineering. Journal*. 10 (4), 415-421.

35. Bai, B., Liu Y., Coste, J.P., & Li, L, C. (2007). Preformed particle gel for conformance control: transport mechanism through Porous media. *SPE Reservoir Evaluation & Engineering. Journal*. 10 (02): 176–184.

36. Cheung, S., Ng, R., Frampton, H., Chang, K. T., & Morgan, J. (2007, March). A swelling polymer for in-depth profile modification: update on field applications. In *SPE Applied Technology Workshop of "Chemical Methods of Reducing Water Production," San Antonia, Texas, USA (pp. 4-6)*.

37. Mustoni, J. L., Denyer, P., & Norman, C. (2010, January). Deep conformance control by a novel thermally activated particle system to improve sweep efficiency in mature waterfloods of the San Jorge Basin. In *SPE Improved Oil Recovery Symposium*. Society of Petroleum Engineers.

38. Wu, Y. S., & Bai, B. (2008, January). Modeling particle gel propagation in porous media. In *SPE Annual Technical Conference and Exhibition*. Society of Petroleum Engineers.

39. Bai, B., Wei, M., & Liu, Y. (2013, March). Field and lab experience with a successful preformed particle gel conformance control technology. In *SPE Production and Operations Symposium*. Society of Petroleum Engineers.

40. Kelland, M. A. (2014). *Production chemicals for the oil and gas industry*. CRC press.

41. Mahdavinia, G. R., Zohuriaan-Mehr, M. J. & Pourjavadi, A. (2004) Modified chitosan III, superabsorbency, salt- and pH-sensitivity of smart ampholytic hydrogels from chitosan-g-PAN. *Polymers for Advanced Technologies*. 15(4): 173-180.

42. Yoshida, R., Uchida, K., Kaneko, Y., Sakai, K., Kikuchi, A., Sakurai, Y. and Okano, T. (1995) Comb-type grafted hydrogels with rapid deswelling response to temperature changes. *Nature*. 374(6519): 240-242.

43. Kaneko, Y., Nakamura, S., Sakai, K., Aoyagi, T., Kikuchi, A., Sakurai, Y. and Okano, T. (1998) Rapid Deswelling Response of Poly(N-isopropylacrylarnide) Hydrogels by the Formation of Water Release Channels Using Poly(ethylene oxide) Graft Chains. *Macromolecules*. 31(18): 6099-6105.

44. Moradi-Araghi, A. (2000). A review of thermally stable gels for fluid diversion in petroleum production. *Journal of Petroleum Science and Engineering*, 26(1), 1-10.

45. Sydansk, R. D. (2011). *Reservoir conformance improvement*. Society of Petroleum Engineers.

46. Sydansk, R. D., & Moore, P. E. (1992). Gel conformance treatments increase oil production in Wyoming. *Oil and Gas Journal;(United States), 90(3)*.

47. Bai, B. J., Huang, F. S., Liu, Y. Z., Seright, R. S., & Wang, Y. F. (2008, April). Paper No. SPE 113997, SPE. In *DOE Symposium on Improved Oil Recovery, Tulsa, Oklahoma, USA*.

48. Bai, B., Li, L., Liu, Y., Wang, Z., & Liu, H. (2004, January). Preformed particle gel for conformance control: factors affecting its properties and applications. In *SPE/DOE Symposium on Improved Oil Recovery*. Society of Petroleum Engineers.

49. Smith, D. D., Giraud, M. J., Kemp, C., McBee, M. S., Taitano, J., Winfield, M., & Everett, D. M. (2006, January). The succesful evolution of Anton Irish conformance efforts. In *SPE annual technical conference and exhibition*. Society of Petroleum Engineers.

50. Pyziak, D., & Smith, D. (2007, November). Update on Anton Irish conformance effort. In *6th international conference on production optimization---reservoir conformance-profile control-water and gas shut-off, Houston*.

51. Imqam, A., Bai, B., Al Ramadan, M., Wei, M., Delshad, M., & Sepehrnoori, K. (2014). Preformed-Particle-Gel Extrusion Through Open Conduits During Conformance-Control Treatments. *SPE Journal*.

52. Yongqiang, T., Jirui, H., & Chenghui, L. (2013). Water shut off in a horizontal well: Lab experiments with starch graft copolymer agent. *Journal of Petroleum Science and Engineering*, 108, 230-238.

53. Qiao, R., & Zhu, W. (2010). Evaluation of modified cationic starch for impeding polymer channeling and in-depth profile control after polymer flooding. *Journal of Industrial and Engineering Chemistry*, 16(2), 278-282.

54. Tongwa, P., Nygaard, R., & Bai, B. (2013). Evaluation of a nanocomposite hydrogel for water shut-off in enhanced oil recovery applications: Design, synthesis, and characterization. *Journal of Applied Polymer Science*, 128(1), 787-794.

55. Zolfaghari, R., Katbab, A. A., Nabavizadeh, J., Tabasi, R. Y., & Nejad, M. H. (2006). Preparation and characterization of nanocomposite hydrogels based on polyacrylamide for enhanced oil recovery applications. *Journal of applied polymer science*, 100(3), 2096-2103.

56. Qiu, Y., Wu, F., Wei, M., Kang, W., & Li, B. (2014, April). Lessons Learned from Applying Particle Gels in Mature Oilfields. In *SPE Improved Oil Recovery Symposium*. Society of Petroleum Engineers.

57. Leslie, T., Xiao, H., & Dong, M. (2005). Tailor-modified starch/cyclodextrin-based polymers for use in tertiary oil recovery. *Journal of Petroleum Science and Engineering*, 46(4), 225-232.

58. Stryer, L. (1995). *Biochemistry 4th ed*. W. H.

59. Amanullah, M., & Yu, L. (2004, January). Dynamic and static fluid loss properties of novel starches prepared using reactive extrusion technique. In *SPE Asia Pacific Oil and Gas Conference and Exhibition*. Society of Petroleum Engineers.

60. Zhang, L. M. (2001). A review of starches and their derivatives for oilfield applications in China. *Starch-Stärke*, 53(9), 401-407.

61. Barrufet, M. A., Burnett, D., & Macauley, J. (1998, January). Screening and Evaluation of Modified Starches as Water Shutoff Agents in Fractures. In *SPE/DOE Improved Oil Recovery Symposium*. Society of Petroleum Engineers.

62. Zhao, F., Hao, H., Hou, J., Hou, L., & Song, Z. (2015). CO_2 mobility control and sweep efficiency improvement using starch gel or ethylenediamine in ultra-low permeability oil layers with different types of heterogeneity. *Journal of Petroleum Science and Engineering*, 133, 52-65.

63. Qiao, R., & Zhu, W. (2010). Evaluation of modified cationic starch for impeding polymer channeling and in-depth profile control after polymer flooding. *Journal of Industrial and Engineering Chemistry*, 16(2), 278-282.

64. Qiao, R., Zhang, R., Zhu, W., & Gong, P. (2012). Lab simulation of profile modification and enhanced oil recovery with a quaternary ammonium cationic polymer. *Journal of Industrial and Engineering Chemistry*, 18(1), 111-115.

65. Bai, B., & Zhang, H. (2011). Preformed-particle-gel transport through open fractures and its effect on water flow. *SPE Journal*, 16(02), 388-400.

66. Bai, B., Zhou, J., Liu, Y., & Tongwa, P. (2013, March). Thermo-Dissoluble Polymer for In-Depth Mobility Control. In *IPTC 2013: International Petroleum Technology Conference*.

67. Schramm, G. (1994). *A practical approach to rheology and rheometry* (pp. 53-56). Karlsruhe: Haake.

68. Chen, Z., Long, Y. F., Schuman P. T., & Bai, B. J., Characterization and Evaluation of Polyacrylamide /Poly (vinyl alcohol) Inter-Penetrating Network Hydrogel for Oil Recovery (*In process*).

69. Bai, B., & Zhang, H. (2011). Preformed-particle-gel transport through open fractures and its effect on water flow. *SPE Journal*, 16(02), 388-400.

70. Smith, D. D., Giraud, M. J., Kemp, C., McBee, M. S., Taitano, J., Winfield, M., & Everett, D. M. (2006, January). The succesful evolution of Anton Irish conformance efforts. In *SPE annual technical conference and exhibition*. Society of Petroleum Engineers.

71. Pyziak, D., & Smith, D. (2007, November). Update on Anton Irish conformance effort. In *6th international conference on production optimization---reservoir conformance-profile control-water and gas shut-off, Houston*.

72. Brattekas, B., Pedersen, S. G., Nistov, H. T., Haugen, A., Graue, A., Liang, J. T., & Seright, R. S. (2014, April). The effect of Cr (III) Acetate-HPAM Gel Maturity on Washout from Open Fractures. In *SPE Improved Oil Recovery Symposium*. Society of Petroleum Engineers.

73. Zhao, J. Z., Jia, H., Pu, W. F., & Liao, R. (2011). Influences of fracture aperture on the water-shutoff performance of polyethyleneimine cross-linking partially hydrolyzed polyacrylamide gels in hydraulic fractured reservoirs. *Energy & Fuels*, 25(6), 2616-2624.

VITA

Yifu Long received his Bachelor of Science degree in petroleum engineering from Northeast Petroleum University in June 2013. He started to pursue his master degree at Department of Petroleum Engineering, Missouri University of Science and Technology from January, 2014. He joined Dr. Baojun Bai's research group from May, 2014 and worked as a research assistant. In December, 2016, he received his degree of Master of Science in Petroleum Engineering from Missouri University of Science and Technology.